



Characterization of T-Circles and Their Formation Reveal Similarities to Agrobacterium T-DNA Integration **Patterns**

Kamy Singer[†], Lan-Ying Lee, Jing Yuan and Stanton B. Gelvin^{*}

Department of Biological Sciences, Purdue University, West Lafayette, IN, United States

OPEN ACCESS

Edited by:

Vladimir Orbovic University of Florida, United States

Reviewed by:

Daisuke Miki. Shanghai Center for Plant Stress Biology, Shanghai Institute for Biological Sciences (CAS), China Yosvanis Acanda Artiga, Simplot, United States

*Correspondence:

Stanton B. Gelvin gelvin@purdue.edu

†Present address:

Kamy Singer, Labcorp Drug Development 6 Moore Drive, Durham, NC, United States

Specialty section:

This article was submitted to Plant Pathogen Interactions, a section of the journal Frontiers in Plant Science

Received: 06 January 2022 Accepted: 29 March 2022 Published: 06 May 2022

Singer K, Lee L-Y, Yuan J and Gelvin SB (2022) Characterization of T-Circles and Their Formation Reveal Similarities to Agrobacterium T-DNA Integration Patterns. Front. Plant Sci. 13:849930. doi: 10.3389/fpls.2022.849930 Agrobacterium transfers T-DNA to plants where it may integrate into the genome. Non-homologous end-joining (NHEJ) has been invoked as the mechanism of T-DNA integration, but the role of various NHEJ proteins remains controversial. Genetic evidence for the role of NHEJ in T-DNA integration has yielded conflicting results. We propose to investigate the formation of T-circles as a proxy for understanding T-DNA integration. T-circles are circular double-strand T-DNA molecules, joined at their left (LB) and right (RB) border regions, formed in plants. We characterized LB-RB junction regions from hundreds of T-circles formed in Nicotiana benthamiana or Arabidopsis thaliana. These junctions resembled T-DNA/plant DNA junctions found in integrated T-DNA: Among complex T-circles composed of multiple T-DNA molecules, RB-RB/LB-LB junctions predominated over RB-LB junctions; deletions at the LB were more frequent and extensive than those at the RB; microhomology was frequently used at junction sites; and filler DNA, from the plant genome or various Agrobacterium replicons, was often present between the borders. Ku80 was not required for efficient T-circle formation, and a VirD2 ω mutation affected T-circle formation and T-DNA integration similarly. We suggest that investigating the formation of T-circles may serve as a surrogate for understanding T-DNA integration.

Keywords: Agrobacterium, Arabidopsis thaliana, Ku80, Nicotiana benthamiana, T-circles, T-DNA integration, VirD2

INTRODUCTION

Agrobacterium tumefaciens is known for its ability to genetically transform plants. During transformation, Agrobacterium transfers a segment of DNA [T (transferred)-DNA] into plant cells where T-DNA may integrate into the plant genome. T-DNA resides on the Agrobacterium tumor inducing (Ti) or rhizogenic (Ri) plasmid which also contains virulence (vir) genes important for transformation. The T-DNA region of Ti/Ri is delimited by two 25 base pair (bp) border repeats, the right and left borders (RB and LB). Natural T-DNAs harbor genes that induce tumors and specify the production of opines, but do not contain genes required for transformation. In modified laboratory strains, T-DNA may be cloned into a binary vector and co-reside with a separate plasmid containing vir genes (Gelvin, 2010, 2017, 2021; Nester, 2015; Singer, 2018; Lacroix and Citovsky, 2019).

1

To initiate T-DNA transfer, VirD2 protein nicks the T-DNA border regions between nucleotides 3 and 4, releasing T-DNA as a single-strand molecule (T-strand) from the Ti/Ri or binary plasmid (Wang et al., 1987). VirD2 remains covalently attached to the 5' end, the RB side, of the released T-strand (Ward and Barnes, 1988; Young and Nester, 1988; Durrenberger et al., 1989; Howard et al., 1989). VirD2 leads the T-strand through a type IV secretion system into the plant cell and the nucleus (Cascales and Christie, 2004; van Kregten et al., 2009). It is thought that after a T-strand enters the plant cytoplasm it is coated by VirE2 to form a T-complex. This proposed complex protects T-DNA and facilitates its trafficking to the nucleus (Howard and Citovsky, 1990; Yusibov et al., 1994; Rossi et al., 1996).

How T-DNA integrates into the plant genome is a major unanswered question of *Agrobacterium*-mediated transformation. One model suggests that T-strands are first converted into double-strand molecules that subsequently integrate. Other models suggest that T-strands invade plant DNA at a nick or double-strand break site, search for microhomology, then use plant proteins to replicate and ligate T-DNA into the genome using plant DNA as a primer (Mayerhofer et al., 1991; Tinland and Hohn, 1995; Tinland, 1996; Tzfira et al., 2004; van Kregten et al., 2016; Gelvin, 2017, 2021). All these models posit that T-DNA integrates into plant genomic nicks or double-strand breaks.

It is likely that integration of T-DNA into plant chromosomes is mediated by host factors. However, the identity of these proteins and their mechanistic roles have yet to be elucidated. On this account, the literature is controversial. Several groups proposed that Ku80 or DNA ligase IV, key components of the classical NHEJ DNA repair pathway, are important for T-DNA integration (Friesner and Britt, 2003; Li et al., 2005; Jia et al., 2012; Mestiri et al., 2014; Saika et al., 2014). Other studies showed no decrease in stable transformation frequency using Arabidopsis ku80 and other NHEJ mutants (Gallego et al., 2003; van Attikum et al., 2003), and two studies noted an increase in stable transformation using NHEJ mutants and Virus Induced Gene Silencing (VIGS) lines (Vaghchhipawala et al., 2012; Park et al., 2015). Similarly, one study indicated an essential role for DNA polymerase θ (PolQ) in T-DNA integration (van Kregten et al., 2016), whereas another study showed that Arabidopsis and rice polQ mutants could be stably transformed, and that the amount of integrated T-DNA was 50-90% of that seen in wild-type plants (Nishizawa-Yokoi et al., 2021).

VirD2 may play a role in T-DNA integration (Tinland et al., 1995). Alteration of four amino acids near the VirD2 C-terminus, termed the omega (ω) domain, to serines almost completely eliminated T-DNA integration while reducing transient transformation only 4-to-5 fold (Shurvinton et al., 1992; Narasimhulu et al., 1996; Mysore et al., 1998). However, the role of the ω domain in T-DNA integration is not clear (Bravo-Angel et al., 1998).

Double-strand circular T-DNA molecules (T-circles) have been isolated from *Agrobacterium*-infected plants (Singer et al., 2012). It is not known if T-circles represent a substrate or replication template for T-DNA integration, or whether they are a dead-end for T-DNA. Evidence from a small number of plant T-circles revealed that extra-chromosomal DNA end-joining occurs *via* a non-homologous pathway (Singer et al., 2012). This study suggested similarities in the mechanism involved in T-circle formation and T-DNA integration.

In this study, we sought additional evidence for similarities between these two processes. We investigated T-circle RB-LB junctions produced under different conditions, including in ku80 plants, or generated using an A. tumefaciensis virD2 ω mutant. These T-circles were formed in N. benthamiana or in Arabidopsis. We determined the DNA sequence at T-circle RB-LB junction sites, the overall T-circle structure, and their rate of formation. Under all conditions tested, T-circles showed similar features to the structure of T-DNA molecules after integration into plant genomes, thus supporting the use of T-circles as a surrogate for T-DNA integration.

MATERIALS AND METHODS

Bacterial Strains and Plasmids, and Plant Material

Plasmids and strains are described in **Supplementary Table 7**. We used Escherichia coli DH10B as the host for all cloning experiments. Agrobacterium tumefaciens EHA105 (Hood et al., 1993) was the host for most transformation experiments. To make a non-polar virD2 mutant of EHA105, we first cloned a 7.2 kbp XhoI fragment containing the virD operon from pEHC13 into the XhoI site of pBluescript ks(+) to generate pE3332. We removed a 3.27 kbp blunted SphI-XhoI fragment from pE3332 and cloned it into SmaI-XhoI digested pE3351 (pBluescript ks(+) lacking a KpnI site) to make pE3353. We replaced the HindIII fragment of pE3353 with a 914bp internal HindIII fragment of virD2 from pE3052, generating pE3355. We removed an internal KpnI fragment of pE3355 to make pE3356. We cloned an XhoI-NotI fragment containing the PvirD-virD1-internal deletion virD2-virD4 into the XhoI-NotI sites of pJQ200sk, generating pE3358. We electroporated pE3358 into A. tumefaciens EHA105, selecting for gentamicin resistance and sucrose sensitivity. We confirmed the resulting resolvent with a virD2 deletion (At1697) by PCR. We linearized pUC18-PvirD-virD1-ω substituted virD2 (pE1500) with EcoRI, blunted it with Klenow fragment, and inserted it into the blunted PstI site of pE1727, generating pE1745. We electroporated pE1745 into A. tumefaciens A136, generating At1132. We mated At1132 with E4 and screened for a strain (At1136) carrying pUC18-PvirD-virD1-ω substituted virD2 on the bacterial chromosome. We isolated pTiEHA105∆virD2 from At1697 and electroporated it into A. tumefacjens At1136, generating At1710. We removed pPH1JI from At1710, generating At1959.

The AMP-ORI and KAN-ORI T-DNA binary vectors were described previously (Singer et al., 2012). The TET-ORI T-DNA binary vector was constructed by PCR amplification of the *TetR* gene using the plasmid pSOUP as the template (Hellens et al., 2000) and primers TetR-EcoRI-F: 5'-atacgaattcctcatgtttgacagcttatcatcg-3' and TetR-PstI-R:

5'-atacctgcagttcttggagtggtgaatccgttag-3', and **PCR** amplification of the ColE1 ori region using the AMP-ORI plasmid as the template and primers ori322: PstI-F 5'-atacctgcagctcatgaccaaaatcccttaacgtgag-3' and ori322-BamHI-5'-atacgaattcggatcccgtattgggcgctcttccgctt-3'. Restriction sites for PstI and EcoRI at the 5' ends of each primer pair were used to ligate the two fragments to generate a plasmid resistant to tetracycline. This plasmid was digested with BamHI and EcoRI and ligated with the BamHI-EcoRI backbone of the AMP-ORI binary vector pE4254 (pRCS11[10-amp]) to replace the ampicillin resistance gene and ori sequence to make pRCS11[TET-ORI (KS101, pE4252)]. This plasmid was further modified by deleting 65 bp between the BamHI and PmeI sites at the RB side and replacing it with a 44 bp synthetic DNA sequence containing an I-SceI site to make pRCS11[TET-ORI] (KS102, pE4253). The following antibiotics were used: For E. coli, ampicillin (100 µg/ml); kanamycin (50 μg/ml); and spectinomycin (50 μg/ml). For A. tumefaciens, spectinomycin (200 μg/ml); kanamycin (50 μg/ ml); and rifampicin (10 µg/ml).

To make the T-DNA binary vector pE4636, we digested pUC19 with *Sac*I and *Sal*I and cloned it into the *Sac*I-*Sal*I site of pE4330, generating pE4579. We cloned a blunted *Sal*I fragment containing the *sacRB* gene from pE1961 into the BstZ171 site of pE4579, generating pE4636.

Nicotiana benthamiana plants were grown as previously described (Singer et al., 2012). Arabidopsis thaliana (ecotype Col-0) and the mutants efr-1 (At5G20480; SALK_044334; Zipfel et al., 2006) and ku80 (At1G48050; SAIL_714_A04) were used. The double mutant ku80/efr-1 was generated by crossing these mutants and screening for homozygous double mutants.

Transformation and T-Circle Isolation

T-circles were isolated from *N. benthamiana* leaves as previously described (Singer et al., 2012). T-circles from *Arabidopsis* were isolated by infecting seedlings using the AGROBEST method (Wu et al., 2014). Expression of β -glucuronidase (GUS) activity in *Arabidopsis* seedlings was measured to monitor transient transformation efficiency, using the T-DNA binary vector pBISN1 (Narasimhulu et al., 1996) and staining with 5-Bromo-4-chloro-3-indolyl- β -D-glucuronide (X-Gluc). *Nicotiana benthamiana* leaves were infiltrated using the *A. tumefaciens* wild-type or *virD2* mutant, discs were cut from infiltrated tissue, stained with X-gluc, and the intensity of staining quantified using ImageJ (US National Institutes of Health).

RESULTS

Experimental Design

We first examined whether DNA patterns present at integrated T-DNA/plant DNA junctions can be found in T-DNA border junctions of T-circles. We recovered and sequenced numerous T-circles using different experimental conditions. For our initial experiments, we used T-DNA constructs containing the *ColE1* origin of replication and a bacterial ampicillin,

tetracycline, or kanamycin resistance gene (Singer et al., 2012; this study), generating the T-DNA constructs AMP-ORI, TET-ORI, and KAN-ORI, respectively (Figure 1A). Binary vectors harboring these constructs were pRCS2 (for KAN-ORI) or pRCS11 (for AMP-ORI and TET-ORI), both of which contain in the plasmid backbone an aadA gene conferring bacterial spectinomycin resistance and the pVS1 origin of replication for maintenance in Agrobacterium (Figure 1B; Singer et al., 2012; this study). Agrobacterium tumefaciens EHA105 containing these constructs were used to infect N. benthamiana and Arabidopsis (Figure 1C). Nicotiana benthamiana was inoculated by leaf agroinfiltration (Singer et al., 2012). We could not obtain T-circles by Arabidopsis leaf agroinfiltration. Instead, we used the AGROBEST method and Arabidopsis efr-1 mutant seedlings (Wu et al., 2014). Following infection, DNA was extracted and used for E. coli transformation. Colonies of transformed E. coli containing T-circles were identified based on the antibiotic resistance encoded by their T-DNA regions (ampicillin, tetracycline, or kanamycin) and their sensitivity to spectinomycin.

RB-LB Junctions in Monomeric T-Circles

Previous studies of T-DNA/plant DNA junctions indicated that deletions occur more frequently and extensively at the T-DNA LB, and that the T-DNA RB is relatively more conserved (Tinland and Hohn, 1995; Tinland, 1996). In addition, microhomologies between T-DNA and plant DNA pre-integration sites often occur, especially near the LB (Windels et al., 2003; Tzfira et al., 2004; Muller et al., 2007; Kleinboelting et al., 2015; Gelvin, 2017, 2021). To examine if similar patterns exist in T-circles, we sequenced RB-LB junctions from T-circles involving a single T-DNA, referred to as monomeric T-circles. In monomeric T-circles the T-DNA RB side (the "head") is ligated to the LB side (the "tail"). Complex T-circles may contain multiple T-DNA copies in various configurations, or large fragments of non-T-DNA regions (Singer et al., 2012).

To identify monomeric T-circles, we screened non-digested plasmid DNA by electrophoresis through agarose gels (**Figure 2**). We also digested T-circle DNA with *Bam*HI, which cuts the T-DNA sequence once (**Figure 2A**). T-circles that were complex by this initial screening were excluded from DNA sequence analysis (**Figure 2A**: Lanes designated "complex," and **Figure 2B**: Lanes 5 and 7). The remainder of the T-circles were sequenced at the junction between the T-DNA RB and LB regions. In several cases DNA sequencing revealed junctions that contained fragments of DNA which are not part of T-DNA. If such fragments were larger than 50 bp, these T-circles were re-classified as complex (**Figure 2B**; Lanes 6 and 9; **Supplementary Figure 1**).

Monomeric T-circles represented 65% (N=211) of those recovered from N. benthamiana (61% of TET-ORI and 68% of AMP-ORI T-circles) and 98% (N =130) of those isolated from $Arabidopsis\ efr$ -1 (**Supplementary Table 1**). Thus, T-circles isolated from N. benthamiana were more frequently complex than were those formed in Arabidopsis.

Sequence analysis of T-DNA junctions from monomeric T-circles showed a prevalence of conserved VirD2 cleavage

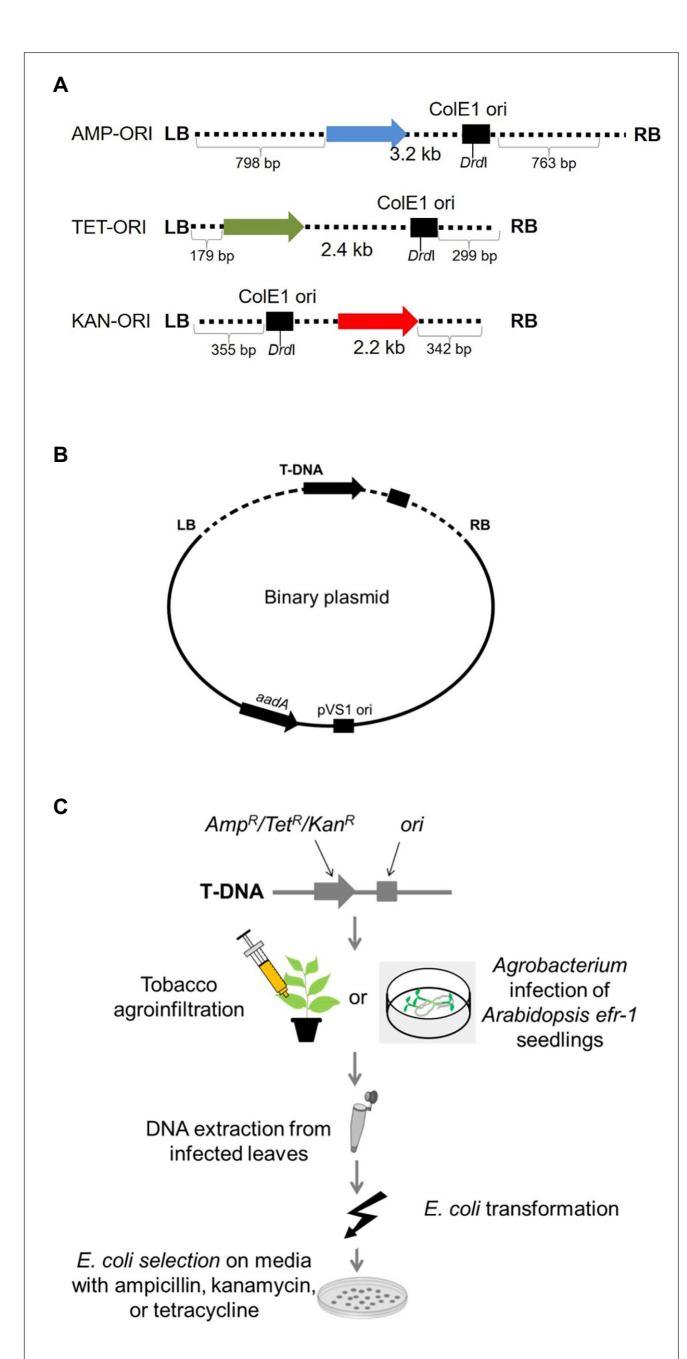


FIGURE 1 | T-circle isolation using "simple" T-circle binary vectors. (A) Schematic diagram of the T-DNA regions of the various T-DNA binary vectors. AMP, TET, and KAN indicated genes encoding ampicillin, tetracycline, and kanamycin resistance, respectively. ORI indicates the CoIE1 origin of replication. LB and RB indicate T-DNA left and right borders, respectively. (B) T-DNA binary vectors used in these experiments. aadA indicates a gene encoding spectinomycin resistance. pVS1 ori indicates the origin of replication of the plasmid in Agrobacterium. (C) Schematic diagram of the plant infection and T-circle isolation processes. Nicotiana benthamiana leaves are infiltrated or Arabidopsis seedlings are co-cultivated with Agrobacterium tumefaciens EHA105 harboring one of the T-circle binary vectors. After 3-6 days, total DNA is extracted from the plant tissue and used to transform E. coli cells. Transformants are selected on medium containing the antibiotic corresponding to the resistance gene in the T-DNA region, then later counterscreened on medium containing spectinomycin. Spectinomycin-sensitive colonies are progressed for T-circle characterization.

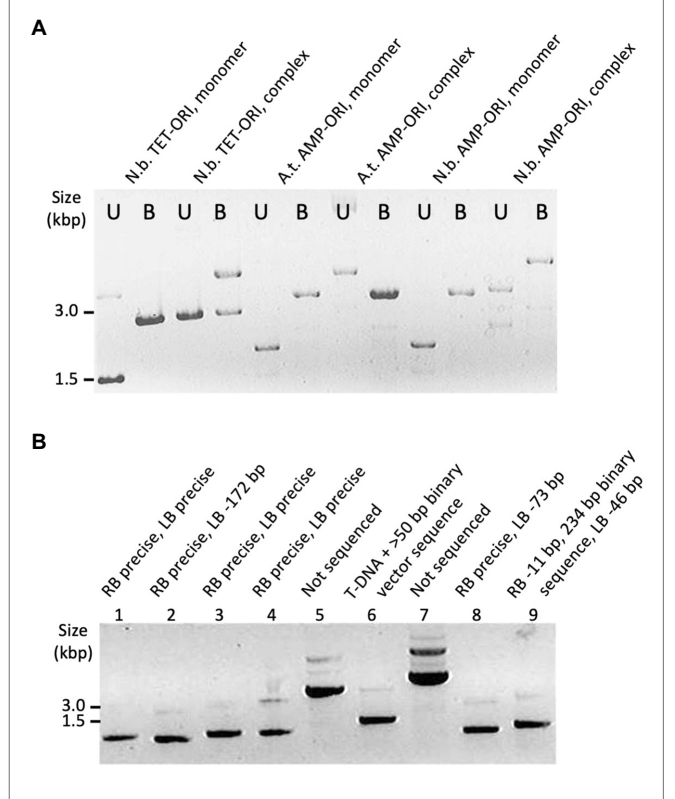


FIGURE 2 | Examples of T-circle analyzed by agarose gel electrophoresis. **(A)** Samples of T-circles either undigested or *Bam*HI digested (U and B, respectively). T-circles were recovered from infected *Nicotiana benthamiana* or *Arabidopsis* plants (N.b. or A.t., respectively, above each lane) using the T-DNA binary vector TET-ORI or AMP-ORI. **(B)** Samples of T-circles (undigested) and the sequencing result for each junction above each lane. T-circles were isolated from *Nicotiana benthamiana* using the TET-ORI binary vector.

positions between nucleotides three and four of the borders (Wang et al., 1987). Such "precise" ends generally occurred more often at the RB side of T-DNA. Using *N. benthamiana* as a host, precise ends occurred in 81% of the RBs and in 48% of the LBs (**Table 1, Supplementary Table 2**). Using *Arabidopsis efr-1*, precise ends occurred in 95% of the RBs and in 92% of the LBs (**Table 1**). Thus, precise ends were more prevalent in T-circles isolated from *Arabidopsis* than from *N. benthamiana*. Whereas precise RBs were frequently ligated to deleted LBs, among 139 precise LBs 138 were ligated to precise RBs (38 precise LBs from *N. benthamiana* and 101 precise LBs from *Arabidopsis efr-1*).

Deletions at RB ends were mostly fewer than 10 nucleotides, and often only 1 or 2 nucleotides. In contrast, most deletions at LBs involved more than 10 nucleotides (**Table 1, Supplementary Tables 2** and **3**). The maximum number of nucleotides deleted from T-DNA ends in T-circles derived from these binary vectors is restricted by the positions of the *ori* and antibiotic resistance genes as these elements are required to recover T-circles (**Figure 1**). Below, we describe a different T-circle binary vector that can support recovery of T-circles with larger deletions.

TABLE 1 Summary of extent of deletions at the RB and LB ends of RB-LB junctions of monomeric T-circles from *Nicotiana benthamiana* and *Arabidopsis thaliana* infected with EHA105.

	Deletion at T-DNA end (bp)							
	Precise	1	2	3–10	11–100	>100	Number of junctions sequenced	
Nicotiana benthamiana								
RB ends	65	3	4	2	4	2	80	
LB ends	38	1	0	1	22	18	80	
Arabidopsis thaliana Col-0								
RB ends	10	0	0	0	0	0	10	
LB ends efr-1	10	0	0	0	0	0	10	
RB ends	106	2	0	1	1	1	111	
LB ends	102	0	0	3	5	1	111	

RB-RB and LB-LB Junctions in Heterodimer T-Circles

Multiple T-DNA molecules often integrate adjacent to each other. We therefore examined RB and LB junctions from T-circles that are made from two different T-DNAs (T-DNA heterodimers).

Figure 3A schematically shows the two possible arrangements of T-circle heterodimers, which can be arranged "head-to-tail" (RB-to-LB) or "head-to-head/tail-to-tail" (RB-to-RB/LB-to-LB). To isolate these heterodimeric T-circles, we co-infiltrated N. benthamiana leaves with Agrobacterium strains containing T-circle TET-ORI or KAN-ORI binary vectors, followed by selection of E. coli colonies on medium containing both tetracycline and kanamycin. We isolated 50 such T-circle heterodimers. To reveal the size and configuration of T-DNAs constituting these T-circles, we determined the sizes of their DrdI restriction endonuclease fragments. Because of potential difficulties in sequencing T-circles made up of more than two T-DNAs, we excluded from our analyses T-circles whose size is greater than that expected from TET-ORI and KAN-ORI heterodimers (4.6 kbp; Figure 3B). DNA sequence analysis of the junctions from these remaining 26 T-circles revealed that 18 were unique, whereas eight were experimental duplicates. From these 18, 16 were arranged "head-tohead"/"tail-to-tail." Only one T-circle was arranged "headto-tail" (Figure 3B T-circle #17). The remaining sequenced T-circle (#12) contained a third short T-DNA fragment (Supplementary Figure 2). Supplementary Figure 3 schematically shows the sequencing results of the various heterodimeric T-circles.

DNA sequence analysis of 32 RBs (from 16 RB-RB junctions) and 28 LBs (from 14 LB-LB junctions) revealed patterns similar to those found at RB-LB junctions of monomeric T-circles (**Table 2** and **Supplementary Table 4**). Among RB-RB junctions 75% of the RBs were precise, similar to 81% of the RBs that were precise in RB-LB junctions. However, none of the LB-LB junctions were precise, in contrast to 48% of the LBs that were precise in RB-LB junctions. In three RB-LB junctions

between KAN-ORI and TET-ORI T-circle heterodimers (two in #17 and one in #12), both the LB and RB ends were precise (Supplementary Table 4).

Microhomology and Filler DNA in T-Circles

Microhomologies between integrated T-DNA sequences and plant pre-integration site sequences at DNA junctions have frequently been observed and associated with repair of DNA double strand breaks (Gorbunova and Levy, 1997; Windels et al., 2003; Tzfira et al., 2004; Muller et al., 2007; Kleinboelting et al., 2015; Gelvin, 2017, 2021). Therefore, we examined patterns of microhomologies at DNA junctions in T-circles.

It should be noted that 12 bp of microhomology can be alleged in all RB-LB junctions with precise ends at both sides. However, the DNA region involved in such potential microhomology resides outside the boundaries of T-DNA from the RB side. Therefore, this microhomology can be involved only if a readthough of the RB had occurred during T-DNA processing in *Agrobacterium*. However, in one T-circle (#022-7) a precise RB and LB were separated by five nucleotides of filler DNA (**Supplementary Table 3**), suggesting that a RB read-through microhomology region is not required for precise RB and LB ends.

Microhomologies were frequent if T-DNA ends were deleted. In RB-LB junctions with deletions at both ends, microhomologies of 1 to 4 nucleotides were present in 6 of 19 junctions (Supplementary Tables 2 and 3). In LB-LB junctions with deletions at both ends, microhomologies of 1 to 6 nucleotides were present in 13 of 14 junctions. In RB-RB junctions all 16 junctions had at least one precise end, with deletions of mostly 1 or 2 nucleotides. Seven of 16 RB-RB junctions contained microhomologies of 1 or 2 bp, but at least three of these are likely not true microhomologies as they are possible only if a read-thorough of a precise RB occurred during T-DNA processing in Agrobacterium (Supplementary Table 4). Overall, LBs show a higher degree of use of microhomologies, similar to what

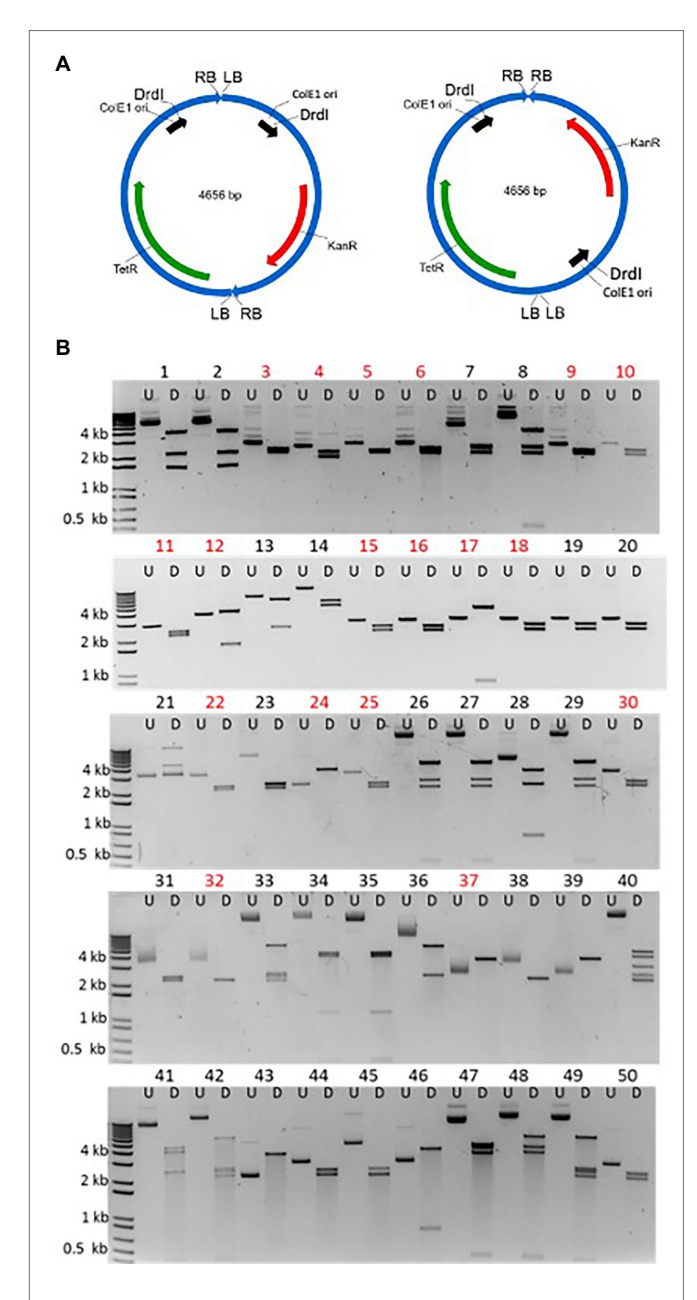


FIGURE 3 | Characterization of T-circles composed of two different T-DNAs. (A) Two T-DNAs can end-join to each other in either of two configurations: "Head-to-tail" that will produce 3.9 and 0.7 kbp *Drd*I fragments (left) or "head-to-head" and "tail-to-tail" that will produce 2.2 and 2.4 kbp *Drd*I fragments (right). (B) 50T-circles conferring resistance to both kanamycin and tetracycline following co-agroinfiltration with *Agrobacterium tumefaciens* EHA105 containing the KAN-ORI and TET-ORI T-DNA binary vectors. Each plasmid is shown undigested (U) and *Drd*I digested (D). Eighteen unique sequenced T-circles are marked in red (T-circles #19, #20, #32, #38, #39, #43, #44, and #50 are duplicates).

has been reported in T-DNA/plant DNA junctions of integrated T-DNAs (Windels et al., 2003; Muller et al., 2007; Kleinboelting et al., 2015).

Filler DNA, defined as short DNA sequences from sources other than sequences directly at the T-DNA or plant DNA

junction site, may occur at T-DNA/plant genome junctions. T-circles may contain filler DNA, mostly 1 to 5 nucleotides in 24 cases (**Table 3**). Among 216 junctions where both the RB and LB were precise, only one included filler DNA. On the other hand, filler DNA was more frequent at junctions involving deleted T-DNA ends. Filler DNA was present in 13 of 36 junctions involving a precise RB with a deleted LB and in 6 of 20 junctions involving deleted RB and LB ends. Filler DNA was also found in LB-LB junctions and RB-RB junctions. Notably, all 16 filler DNAs next to precise RBs were either A or T nucleotides (**Table 3**).

Plant DNA, *Agrobacterium* Chromosomal DNA, and *Agrobacterium* Plasmid DNA in T-Circles

Most filler DNAs at T-DNA/plant genome junctions comprise short sequences of T-DNA or sequences from the binary vector backbone (Simpson et al., 1982; Kononov et al., 1997; Wenck et al., 1997). Some T-DNA insertions may include plant DNA sequences from sites different from the site of insertion (Kleinboelting et al., 2015). DNA from both the *Agrobacterium* chromosomes and from other *Agrobacterium* replicons (Vir helper plasmids, the "cryptic" plasmid pAtC58, non-T-DNA sequences of the Ti-plasmid, etc.) have been reported at T-DNA insertion sites (Ulker et al., 2008; Nishizawa-Yokoi et al., 2021).

Some of the sequenced T-circles contained additional DNA between the sequenced borders (**Table 4**; **Supplementary Figure 3**). The DNA sequences in these T-circles was in many cases homologous to internal T-DNA regions or to the binary vector backbone, as previously reported (Singer et al., 2012). In addition, a 375 bp fragment of *Agrobacterium* chromosomal DNA was found in T-circle #052-44, whereas larger fragments of *Agrobacterium* Ti-plasmid DNA were found in T-circles #052-22 and #052-66. *Nicotiana benthamiana* DNA was found in T-circles #008-73 and #052-18 (290 bp and 188 bp, respectively). Thus, different types of DNA, that have previously been identified at T-DNA/plant DNA junctions in transgenic plants, can also be found between T-circle borders.

Generation of T-Circles Using an Improved T-circle Binary Vector

The T-circle binary vectors used for our initial experiments all contain a small T-DNA region with only sequences important for replication and antibiotic selection in *E. coli*. Because both of these elements are essential for T-circle rescue, large T-DNA border deletions could not be tolerated. Extensive time-consuming counter-screening was required to differentiate between true T-circles and contaminating binary vector sequences, which represent the large majority of antibiotic-resistant *E. coli* transformants.

We therefore constructed a new T-circle binary vector (pE4636) to a meliorate these problems. The new plasmid contains within the T-DNA region a ColE1 ori sequence and a β -lactamase (ampicillin-resistance) gene. We positioned

TABLE 2 | Summary of extent of deletions in T-circle heterodimers at the RB and LB ends of RB-RB and LB-LB junctions isolated from Nicotiana benthamiana.

		Deletion at T-DNA end (bp)						
	Precise	1	2	3–10	10–100	>100	Number of junctions sequenced	
RB ends	24	4	2	0	1	1	32	
LB ends	0	0	0	0	22	6	28	

TABLE 3 | Filler DNA from unknown source at T-DNA junctions.

T-DNA junction	Number of Junctions	Junctions with filler DNA	Filler DNA
Precise RB- Precise LB	216	1	TAATA
Precise RB- Deleted LB	36	13	T, T, A, A, AAAA, T, A, T, A, A, A, T, A
Deleted RB- Deleted LB	20	6	A, GT, AGCT, G, A, GTC
Deleted RB- Precise LB	1	1	TTAATAGTTTAAACTGAAGCGCAGAT
Precise RB- Precise RB	9	2	ATA, A
Precise RB- deleted RB	8	0	
Deleted LB- Deleted LB	14	1	A

a plant-active *Venus-intron* gene next to the β -lactamase gene, and a plant-active hptII gene next to the LB. We also placed within the vector backbone sequence a sacB gene. This new T-circle binary vector allowed us to monitor plant transient transformation (Venus fluorescence) and stable integration of T-DNA into the plant genome (hygromycin resistance). The sacB gene allowed for negative selection of transformed $E.\ coli$ cells containing the entire binary vector rather than T-circles (sucrose sensitivity). Importantly, the hptII and Venus-intron genes near the LB allowed for detection of large LB deletions without disrupting sequences essential for T-circle recovery in $E.\ coli$. Figure 4 shows maps of this new binary vector and the full-size T-circle that it could generate.

We used this new T-circle binary vector to obtain T-circles from infiltrated *N. benthamiana* leaves. Isolated T-circles were first digested with *SalI* to determine their size and whether sequences more than 76 bp from the RB remained intact. We used *PvuII* digestion to determine if DNA sequences more than 273 bp from the RB remained intact. If either of these sites remained intact, we sequenced across the RB-LB interface using primers set back from the RB. If neither of these two sites existed, we subjected the T-circle plasmids to WideSeq analysis to determine their entire sequence.

Of the 42 T-circles characterized, sequences extending to and through the RB region were generated by Sanger

sequencing for 30 T-circles. An additional 12 T-circles were completely sequenced using WideSeq. The data are summarized in Table 5 and in Supplementary Table 5. In total, 23 T-circles (55%) contained a precise RB, whereas none contained a precise LB. Microhomology was found in 13 T-circles (31%) at the RB region and seven T-circles (17%) at the LB region. The LB region frequently showed long deletions, extending from a few hundred bases to >5.9 kbp. Long regions of filler DNA were found in nine T-circles (21%), and an additional four T-circles contained a few bp of filler DNA between the borders. These filler DNAs derived from N. benthamiana, the "cryptic" plasmid pAtC58, or from the binary vector (Supplementary Table 5). More than one third of the T-circles (15; 36%) contained major rearrangements, including binary vector or T-DNA sequences in an inverted orientation, or other major sequence rearrangements of unknown origin.

T-circles derived from the new T-DNA binary vector resembled those derived from the simpler binary vector. However, the long "buffer" of T-DNA sequences adjacent to the LB allowed us to recover large LB deletions and sequence rearrangements.

Ku80 Is Not Required for T-Circle Formation in Plants

We tested if the classical NHEJ pathway were involved in T-circle formation by examining the rate of T-circle formation and patterns of DNA end-joining at junctions of T-circles in an *Arabidopsis ku80/efr-1* double mutant. The *efr-1* mutant allows higher transient transformation of *Arabidopsis* (Zipfel et al., 2006).

Arabidopsis ku80/efr-1 and control efr-1 seedlings were infected with Agrobacterium containing the AMP-ORI construct. DNA was extracted and used for E. coli transformation. Under our conditions, 82 of 516 (15.9%) and 75 of 475 (15.8%) of the amp-resistant E. coli colonies isolated from efr-1 and ku80/efr-1 plants, respectively, were sensitive to spectinomycin, as expected from colonies that contain T-circle, rather than binary vector, DNA. Therefore, Ku80 deficiency did not affect the rate of T-circle formation. We sequenced 63 RB-LB junctions from T-circles recovered from ku80/efr-1 (Supplementary Table 6). Most junctions at both the LB and RB were precise, as was found in T-circles recovered from control efr-1 plants. Therefore, Ku80 deficiency did not result in differences in either the rate of formation or T-DNA border patterns of T-circles.

TABLE 4 | Sequenced T-DNA junctions of complex T-circles.

Sample no.	Strain	Construct	RB*	Microhomology ^a	Filler DNA ^b	Microhomology°	LB*
Nicotiana benth	amiana						
#002–23	EHA105	TET-ORI	Readthrough >380 bp	NA	NA	NA	NA
#003–50	EHA105	TET-ORI	Precise	2 (GA)	236 bp binary +9 bp internal T-DNA sequence	0	-72
#003–61	EHA105	TET-ORI	– 1	2 (TG)	>486 bp binary sequence	NA	NA
#003–62	EHA105	TET-ORI	Precise	4 (TTGA)	>489 bp binary sequence	NA	NA
#003–64	EHA105	TET-ORI	Precise +1	0	>202 bp internal T-DNA sequence	NA	NA
#008–73	EHA105	TET-ORI	Precise	1 (A)	290 bp plant DNA	6 (TCAGGC)	-11
#009–12	EHA105	TET-ORI	Precise +4	5 (CAGGC)	>585 bp binary sequence	NA	NA
#050–14	EHA105	AMP-ORI	Readthrough 151 bp	NA	0	0	-215
#050–23	EHA105	AMP-ORI	Precise	0	>431 bp binary sequence	NA	NA
#052–9	EHA105	AMP-ORI	Precise+1	1 (C)	284 bp binary sequence	3 (AGC)	-456
[‡] 052–17	EHA105	AMP-ORI	Readthrough 224 bp	NA	0	0	-237
#052-18	EHA105	AMP-ORI	-21	4 (TTCA)	188 bp plant DNA	0	-239
#052–22	EHA105	AMP-ORI	Precise +1	0	>406 bp Ti plasmid sequence	NA	NA
#052–28	EHA105	AMP-ORI	Precise	0	84 bp T-DNA sequence	3 (GCT)	-436
#052–35	EHA105	AMP-ORI	Precise	0	>484 bp binary sequence	NA	NA
#052–44	EHA105	AMP-ORI	Precise+1	1 (C)	375 bp <i>Agrobacterium</i> chromosomal DNA	3(CGA)	-317
#052-45	EHA105	AMP-ORI	Readthrough 129 bp	NA	0	3 (TTT)	-714
#052–55	EHA105	AMP-ORI	Precise	2 (GA)	74 bp internal T-DNA sequence	2(GG)	-683
#052-60	EHA105	AMP-ORI	Precise +2	2 (CA)	>560 bp binary sequence	NA	NA
#052-63	EHA105	AMP-ORI	Readthrough 192 bp	NA	0	0	-265
#052–66	EHA105	AMP-ORI	Precise	0	>799 bp Ti plasmid sequence	NA	NA
/irD2ω							
#005–8	At1959	TET-ORI	-11	0	234 bp binary sequence	4 (AACA)	-46
Arabidopsis Co	I-O					,	
#021–4	EHA105	AMP-ORI	Readthrough >461 bp	NA	NA	NA	NA

NA, not available. *Right border (RB) and left border (LB) numerical values represent the position in the DNA relative to the precise end.

T-Circles Generated Using an Agrobacterium VirD2 ω Mutant Form Less Frequently Than Do T-circles Generated Using a Wild-Type Agrobacterium Strain

A substitution mutation in the omega (ω) domain of VirD2 (Shurvinton et al., 1992) severely reduces (>95%) T-DNA integration while only reducing T-DNA transfer into plant cells by ~75–80% (Mysore et al., 1998). We generated an A. tumefaciens EHA105 derivative (At1959) that contains this virD2 mutation. We first indirectly examined the rate of T-DNA transfer by this mutant strain by measuring transient β-glucuronidase (GUS) expression, conferred by a gusA-intron gene within T-DNA (pBISN1). We agroinfiltrated N. benthamiana leaves with wild-type (At2120) and mutant Agrobacterium (At2121 or At2162) at low cell density (~106 and ~105 cfu/ml) to avoid a saturation response (**Figure 5**). T-DNA transfer from the virD2 ω mutant was 7.5–9.1% that of T-DNA transfer from the wild-type VirD2 strain.

We next infiltrated *N. benthamiana* leaves with *Agrobacterium* strains harboring the AMP-ORI or TET-ORI

T-DNA binary vectors. Infection using the wild-type strain resulted in 144 of 1,118 (12.9%) colonies that were resistant to ampicillin or tetracycline but sensitive to spectinomycin. However, using the virD2 ω mutant only 12 of 3,450 (0.35%) of the transformed E. coli colonies were resistant to ampicillin or tetracycline but sensitive to spectinomycin. Therefore, the rate of T-circle formation obtained using the virD2 ω mutant Agrobacterium strain was 2.7% (0.35/12.9) of that obtained using Agrobacterium strains with a wild-type VirD2 gene.

DNA sequence analysis of RB-LB junctions showed that LB T-circle sequences derived from inoculation with the virD2 ω mutant were similar to those obtained using a wild-type VirD2 Agrobacterium strain (**Table 6**). However, RB sequences from six T-circles derived from use of the virD2 ω mutant strain were all precise, as opposed to our previous finding of only 81% precise RBs using a wild-type Agrobacterium strain. To obtain more examples of T-circles generated using the virD2 ω mutant Agrobacterium strain, we infiltrated N. benthamiana leaves with A. tumefaciens At2332, a virD2 ω mutant (At1959) containing the new T-circle binary vector pE4636. DNA sequence

^aMicrohomology between RB and filler DNA.

^bFiller DNA is defined here as any DNA sequence not part of the contiguous T-DNA.

[°]Microhomology between filler and LB.

TABLE 5 | Summary of properties of T-circles from *Nicotiana benthamiana* generated by pE4636.

Number	Precise RB	Precise LB ^a	Microhomology at RB region	Microhomology at LB region	Filler DNA	Major rearrangements
42	23 (55%)	0 (out of 39; 0%)	13 (31%)	7 (17%)	2 (plant; 5%) 3 (pAtC58; 7%) 4 (binary; 10%) 4 (few bp; 10%)	Binary vector or T-DNA reverse complement or other unknown rearrangement (15; 36%)

aln some instances, Sanger sequencing did not extend far enough to obtain a LB region sequence if there were a large filler. For some plasmids, Wide-seq analysis revealed the entire T-circle sequence.

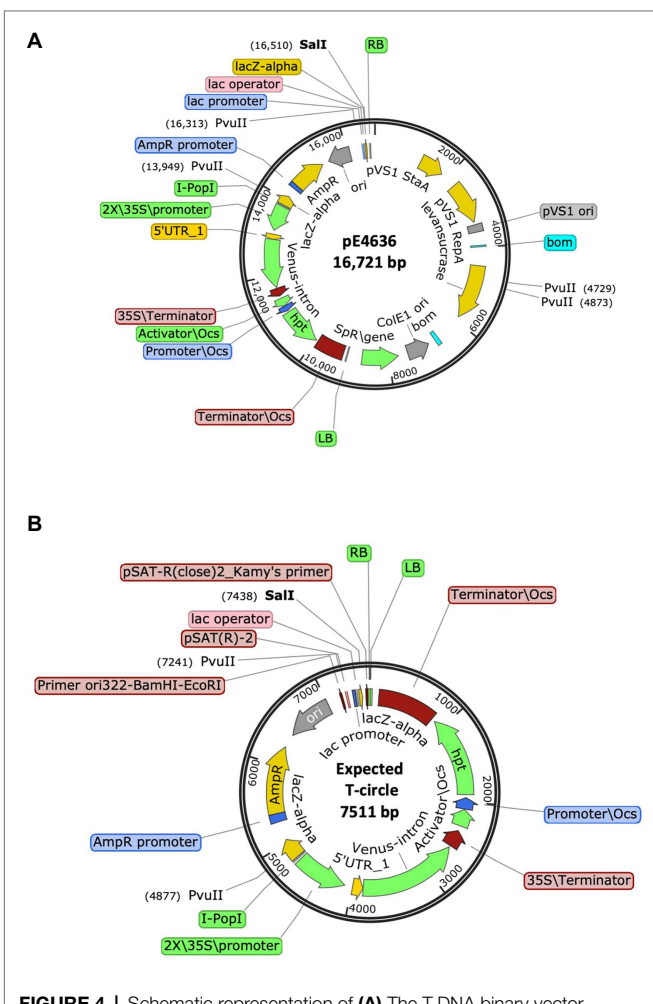


FIGURE 4 | Schematic representation of **(A)** The T-DNA binary vector pE4636, and **(B)** The expected T-circle formed from this plasmid by joining of the T-DNA right and left borders (RB and LB, respectively).

analysis of 17T-circle RB-LB junctions again indicated only precise RBs. In addition, LBs in T-circles generated by the virD2 ω mutant Agrobacterium strain were more frequently precise than those obtained using Agrobacterium strains containing a wild-type VirD2 gene (42% vs. 0%; **Tables 5** and **6**). Thus, the VirD2 ω mutation altered the use of both RBs and LBs in T-circles, indicating that VirD2 is involved in T-circle formation.

T-Circles Form in planta but Not in Agrobacterium

We previously showed that T-circles cannot be recovered when plants are infiltrated with a virB mutant Agrobacterium strain, indicating that T-circles are formed in planta. We also showed that T-circles do not result from ligation of T-DNA molecules after transformation into E. coli (Singer et al., 2012). Two studies had previously indicated that circular T-DNA molecules could form in Agrobacterium as a result of recombination between similar sequences in the T-DNA LB and RB regions (Koukolikova-Nicola et al., 1985; Machida et al., 1986). To test whether the T-circles we observed had formed by recombination in Agrobacterium, we investigated T-circle heterodimer formation in Agrobacterium. Agrobacterium strains individually containing the KAN-ORI or TET-ORI binary vectors were co-infiltrated into N. benthamiana leaves. After 6 days, 50 mg of plant tissue was crushed in sterile LB medium and plated onto solidified YEP medium containing either spectinomycin, kanamycin, tetracycline, or kanamycin plus tetracycline. Agrobacterium colonies appeared on YEP medium containing kanamycin or tetracycline, but not on medium containing both kanamycin and tetracycline. Furthermore, we tested colonies that grew on tetracycline (n = 158), kanamycin (n = 102), or spectinomycin (n = 275). None of these colonies grew on medium containing both kanamycin and tetracycline. These results indicate that recombination between the KAN-ORI and TET-ORI T-DNA regions did not occur in Agrobacterium.

To show that T-circle heterodimers had formed *in planta* during these infiltrations, total DNA was extracted from co-Agroinfiltrated leaves and used to transform *E. coli*. From 192 colonies selected on kanamycin, 64 were spectinomycinsensitive, indicating T-circle formation. Of these, seven were also tetracycline-resistant, indicating T-circle heterodimer formation. Similarly, from 190 colonies selected on tetracycline, 42 were spectinomycin-sensitive and seven of these were also kanamycin-resistant, again indicating T-circle heterodimer formation. Thus, in total 4.7% of the *E. coli* colonies selected on either kanamycin or tetracycline were resistant to both antibiotics.

The results of these experiments indicate that we could recover T-circle heterodimers from Agro-infiltrated *N. benthamiana* leaves but could not detect recombination between these same T-DNA regions in *Agrobacterium* cells.

DISCUSSION

Nicking of the T-DNA border sequences by VirD2 releases a T-strand containing border nucleotides 1-3 at the RB and nucleotides 4-25 at the LB. Before or during the process of T-DNA integration into the plant genome, alterations of T-DNA commonly occur. These include resection of T-strands at the LB and/or RB ends. In addition, filler DNA may occur at T-DNA/plant DNA junctions; this filler may come from within T-DNA or from the plant genome (Kleinboelting et al., 2015). Filler DNA may also originate from other Agrobacterium replicons, including bacterial chromosomal DNA or other bacterial plasmids (Ulker et al., 2008; Nishizawa-Yokoi et al., 2021). Microhomologies between T-DNA border region sequences and plant pre-integration sequences may occur; these are generally more prevalent near the LB (Windels et al., 2003; Tzfira et al., 2004; Muller et al., 2007; Kleinboelting et al., 2015; Gelvin, 2017, 2021). T-DNA may integrate into plant DNA as a monomer, as dimers (RB-to-LB [head-to-tail], RB-RB [head-to-head], or LB-LB [tail-to-tail]), or as multimers. Finally,

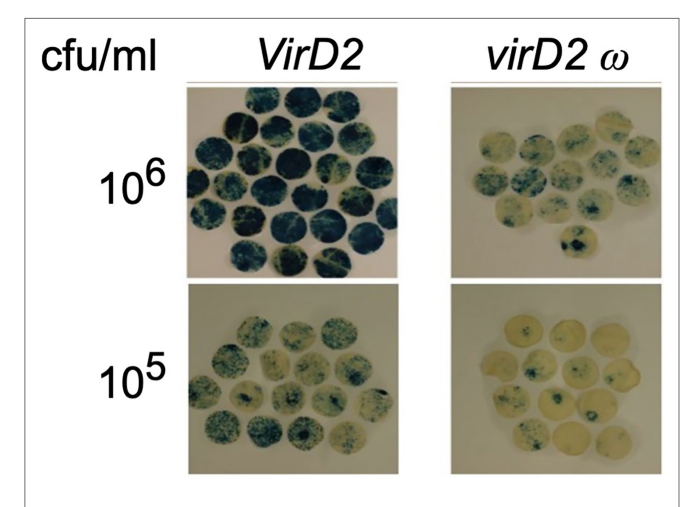


FIGURE 5 | Transient expression of GUS activity in *N. benthamiana* leaves agroinfiltrated with *Agrobacterium* containing a wild-type *VirD2* gene (left panels) or the *virD2* ω mutant (right panel). *Agrobacterium tumefaciens* containing a wild-type *virD2* gene, the AMP-ORI T-circle binary vector, and the T-DNA binary vector pBISN1 or a similar strain with the ω mutant *virD2* gene were infiltrated at the indicated concentration. Discs cut from leaves after 4 days were stained with X-gluc, cleared with 70% ethanol, and the relative staining intensity calculated using ImageJ software. cfu, colony forming units.

integration of T-DNA frequently causes major plant chromosome rearrangements (Castle et al., 1993; Nacry et al., 1998; Tax and Vernon, 2001; Lafleuriel et al., 2004; Curtis et al., 2009; Clark and Krysan, 2010; Majhi et al., 2014; Ruprecht et al., 2014; Hu et al., 2017; Jupe et al., 2019). These different DNA patterns at T-DNA/plant DNA junctions comprise the foundations for models explaining possible mechanisms of T-DNA integration (reviewed in Tzfira et al., 2004; Gelvin, 2017, 2021; Singer, 2018).

The mechanism of T-DNA integration into the plant genome, and whether various plant DNA repair pathways and specific proteins play roles in it, remains highly controversial, with many different theories and conflicting results. Homologous recombination is not used for T-DNA integration; despite large regions of homology between sequences within T-DNA and plant DNA, targeting using homology is extremely rare in plants, although it is common in yeast (Rolloos et al., 2014, 2015). Among the non-homologous end-joining (NHEJ) pathways, both the "classical" (Ku-dependent; cNHEJ) and the microhomology-mediated (MMEJ) end-joining pathways have been suggested to promote T-DNA integration (Mayerhofer et al., 1991; Tinland and Hohn, 1995; Tinland, 1996; Tzfira et al., 2004; van Kregten et al., 2016; Gelvin, 2017, 2021). Genetic experiments to determine T-DNA integration pathway components have involved ablation of specific cNHEJ and/ or MMEJ components, followed by quantitation of stable transformation frequencies, usually by antibiotic/herbicide selection of transgenic events. Some of these studies reported a decrease in stable transformation using ku70/80 or DNA ligase IV (lig4) mutants, suggesting involvement of the cNHEJ pathway in T-DNA integration (Friesner and Britt, 2003; Li et al., 2005; Jia et al., 2012; Mestiri et al., 2014; Saika et al., 2014). Other studies showed little or no difference among stable transformation frequencies using cNHEJ or MMEJ mutants (Gallego et al., 2003; van Attikum et al., 2003). Still other studies showed that mutation or down-regulation of ku70/80, xrcc4, or DNA ligase VI (lig6) increased the frequency of stable transformation (Vaghchhipawala et al., 2012; Park et al., 2015). Most of these studies suffered from the limitations of using stable transformation (with selection) as a proxy for T-DNA integration (see discussion in Gelvin, 2021). However, some studies examined T-DNA integration biochemically in the absence of selection (Vaghchhipawala et al., 2012; Park et al., 2015; Nishizawa-Yokoi et al., 2021). These latter studies indicated that mutation of cNHEJ and

TABLE 6 | T-DNA junctions of T-circles from Agrobacterium benthamiana using virD2 ω mutant Agrobacterium strains.

Number characterized	Strain	Construct	Precise RB	Precise LB ^a	RB Microhomology	LB Microhomology ^a	Filler DNA
6	At1959	TET-ORI or	6 (100%)	3 (50%)	1 (17%)	0	1
18	At2332	AMP-ORI pE4636	18 (100%)	5 (of 12; 42%)	5 (28%)	2 (of 13; 15%)	(1 bp, A) 6 (pAtC58)
							3 (linear chromosome)

^aIn some instances, Sanger sequencing did not extend far enough to obtain a LB region sequence if there were a large filler. For some plasmids, Wide-seq analysis revealed the entire T-circle sequence.

MMEJ genes did not substantially decrease the amount of T-DNA integrated into the plant genome and may, in some instances, increase it. The initially reported requirement for DNA polymerase θ , an essential component of MMEJ, to obtain stable transformants (van Kregten et al., 2016) has been disputed (Nishizawa-Yokoi et al., 2021). Thus, the participation of various NHEJ pathways and individual components of these pathways remains highly controversial, and genetic approaches to solving this conundrum may be limited if proteins required for T-DNA integration are essential for cellular viability (Gelvin, 2021).

We propose that studying the formation of T-circles will inform us about T-DNA integration. However, we first needed to show that T-circle border junctions resembled T-DNA/plant DNA junctions, and that factors which influence T-DNA/plant DNA junctions similarly influence T-DNA border junctions in T-circles. We therefore sequenced hundreds of T-circle border junctions, generated in both wild-type N. benthamiana and in Arabidopsis, and generated in an Arabidopsis ku80 cNHEJ mutant. We also examined the amount of T-circles formed and the precision of LBs and RBs following infection by an Agrobacterium VirD2 ω mutant. The results of these studies indicated that in all aspects examined, T-circle border junctions resembled what has been well documented with T-DNA/plant DNA junctions.

The Structure of T-DNA Border Junctions in T-Circles Resembles T-DNA/Plant DNA Junctions

Within Agrobacterium, T-strands retain, at the LB, nucleotides 4-25 of the 25 bp border repeat, whereas the RB contains nucleotides 1-3 covalently linked to VirD2 (Wang et al., 1987; Ward and Barnes, 1988; Young and Nester, 1988; Durrenberger et al., 1989; Howard et al., 1989). A "simple" and "precise" integration of T-DNA into plant DNA would result in plant DNA joined to one T-DNA molecule, using nucleotides 4-25 at the LB and nucleotides 1-3 at the RB. Such ideal T-DNA insertions are rarely observed. Rather, multiple copies of T-DNA often integrate next to each other in RB-LB, RB-RB, or LB-LB orientation (Windels et al., 2003; Muller et al., 2007). Deletions of plant DNA at the integration site frequently exist, and T-DNA deletions at the borders are common. T-DNA border deletions are especially prevalent and may be large at the LB, which is not protected by VirD2, but may also occur at the RB (Durrenberger et al., 1989; Windels et al., 2003; Kleinboelting et al., 2015). "Filler" DNA may appear at the borders. This filler DNA may be from within T-DNA, from other regions of the Ti-plasmid (or the binary vector backbone), Agrobacterium chromosomal DNA, or DNA from other Agrobacterium replicons (Muller et al., 2007; Ulker et al., 2008; Nishizawa-Yokoi et al., 2021). Filler DNA from the plant genome usually derives from sequences nearby, or on the same chromosome, as the T-DNA integration site, although sequences from other chromosomes may be used (Kleinboelting et al., 2015). Finally, microhomology between T-DNA borders (or deleted borders) and sequences immediately upstream of the integration site is frequent, especially at the LB (Windels et al., 2003; Muller et al., 2007; Kleinboelting et al., 2015). This resulting picture of junctions at T-DNA integration sites suggests the use of microhomology to "copy in" other DNA sequences by a DNA polymerase template switching mechanism (Kent et al., 2016; van Kregten et al., 2016; Wyatt et al., 2016; Schimmel et al., 2017; Nishizawa-Yokoi et al., 2021).

Our analyses of hundreds of T-circles indicated that, collectively, all the properties of T-DNA/plant DNA junctions could be recapitulated by examining RB-LB junctions of T-circles. T-circles could be "complex," resulting from linkage of multiple T-DNAs in either RB-LB configuration or in RB-RB/LB-LB configuration. T-DNA border deletions occur frequently, and are generally more extensive at the LB than at the RB. Use of the binary vector pE4636 indicated that deletions at the LB can be up to ~5 kbp (deletions at the RB>~500 bp would not be tolerated in our T-circle recovery system because they would delete the *ColE1* origin of replication necessary to recover T-circles in E. coli). Filler DNA coming from various Agrobacterium and plant sources could occur between the RB and LB regions. Because T-circles are not integrated into plant DNA, the occurrence of plant DNA sequences in T-circles indicates that such plant DNA sequences are "copied" into the T-circles after arrival of T-strands in the nucleus. It is not clear how DNA from other Agrobacterium replicons links to T-circle sequences. Such linkage could occur in Agrobacterium prior to T-DNA transfer or could occur in the plant if these sequences were mobilized into the plant nucleus. Preliminary analysis of these Agrobacterium sequences indicates that they are not flanked by a consensus VirD2 cleavage site. Finally, microhomology frequently occurred between T-DNA (at or near the borders) and filler DNA, or the ends of deletions in T-DNA. Use of microhomology is an indication of a MMEJ process, perhaps using DNA polymerase θ .

Use of *Agrobacterium* **and Plant Proteins for T-Circle Formation**

Although VirD2 protein remains attached to T-strands as they enter the nucleus, the role, if any, for VirD2 in T-DNA integration remains unknown. VirD2 is involved in many processes upstream of T-DNA integration, and mutations in VirD2 that decrease integration may also be impaired in one or more of these processes. Despite these potential complications, Tinland et al. (1995) showed that alteration of VirD2 arginine¹²⁹ to glycine affected the precision of insertion of T-DNA into plant DNA; this mutation resulted in more deletions at integrated RBs. Mysore et al. (1998) showed that substitution of four serine residues for the VirD2 ω region sequence DDGR did not alter the general pattern of T-DNA integration, but preferentially decreased the extent of T-DNA integration (as measured by stable transformation) relative to transient transformation. Our studies on T-circles generated using an Agrobacterium strain with the virD2 ω mutation indicated that the frequency of

T-circle formation was 2.7% that of T-circles formed using an Agrobacterium strain containing a wild-type VirD2 gene. These data correlate well with past estimates of the decrease in T-DNA integration using this virD2 ω substitution mutant (Mysore et al., 1998). In addition, the precision of RBs (and to a lesser extent, LBs) in T-circles generated using the *virD2* ω substitution mutant was different from those generated using a wild-type VirD2 gene: All of the 23 T-circles examined from N. benthamiana using the virD2 ω substitution mutant contained precise RBs, whereas a lower percentage of T-circles derived using a wildtype VirD2 Agrobacterium strain contained precise RBs (81% using the initial T-circle binary vectors, 53% using the new T-circle binary vector pE4636). A lack of extensive RB deletions using the VirD2 ω mutant was previously noted (Mysore et al., 1998). Taken together, these data indicate that VirD2 protein, and especially the ω domain, influence the precision of both RBs and LBs in T-circles, and by extrapolation in T-DNA integration. The VirD2 ω mutant protein may remain on the T-strand longer than does wild-type VirD2 during T-circle formation, thus protecting it more extensively from nuclease degradation. Alternatively, the VirD2 ω mutant protein may block the activity of proteins involved in microhomology searching near the borders. Future experiments will examine these possibilities.

The role of Ku80 in T-DNA integration is controversial, as described above. Using a *ku80* mutant *Arabidopsis* line, we showed no decrease in the frequency of T-circle formation. Neither did we find any major differences among T-circles generated in wild-type vs. *ku80* mutant *Arabidopsis* plants with regard to their RB-LB junctions. These results are consistent with the model that Ku80, and therefore the cNHEJ pathway, is not essential for either T-circle formation or for T-DNA integration.

T-Circles and T-DNA Integration

T-strands enter the plant nucleus as single-strand molecules (Tinland et al., 1994; Yusibov et al., 1994) that can be converted to double-strand linear or double-strand circular molecules. It is not known which of these three forms of T-DNA serve as the substrate, or replication template in the case of single-strand molecules, for integration. Double-strand circular T-DNA molecules have been isolated from *Agrobacterium*-infected yeast cells (Bundock et al., 1995; Rolloos et al., 2014). Examination of the border regions of these circles indicated that they were always precise, with nucleotides 1–3 of the RB linked to nucleotides 4–25 of the LB. Thus, studying T-circles isolated from yeast may not serve as a good model for T-DNA integration in plants.

Bakkeren et al. (1989) inserted a Cauliflower Mosaic Virus (CaMV) replicon in a T-DNA region of a binary vector. Infection of tobacco plants by *Agrobacterium* containing this binary vector resulted in circular CaMV replicons joined at or near the T-DNA borders. Analysis of these border region junctions indicated structures similar to what has been seen at T-DNA/plant DNA junctions: RBs were near-precise, and more extensive deletions occurred at the LB. Short "filler" DNA sequences between the border regions were

seen in about one third of the molecules. These T-DNA border characteristics are similar to what we saw in our extensive T-circle analyses.

One peculiarity of our results was the different complexity of T-circles isolated from *N. benthamiana* and *Arabidopsis*. T-circle molecules isolated from *N. benthamiana* were frequently complex, with extensive DNA deletions, rearrangements, and filler DNA occurring at or near the border junctions. T-circles isolated from *Arabidopsis* were mostly simple T-DNA monomers with precise RB and LB junctions. It is not clear whether these differences reflect the disparate host plant species used or the different methods of *Agrobacterium* infection. Leaf infiltration of *Arabidopsis* remains very inefficient, although a recent protocol shows improvement of *Arabidopsis* leaf infiltration efficiency (Zhang et al., 2020). We are currently attempting to isolate T-circles from *Arabidopsis* leaves using a modification of this method.

Although the T-circle border junctions that we and others (Bakkeren et al., 1989) have examined closely resemble the range of border junction characteristics seen in integrated T-DNA molecules, we cannot argue that T-DNA circles are the substrate for integration into plant DNA. Rather, we propose that investigation of the mechanism of T-circle formation in plants may serve as a proxy for studying the events, and molecules, involved in T-DNA integration.

DATA AVAILABILITY STATEMENT

The datasets presented in this study can be found in the online repository NCBI GenBank under the accession numbers BankIt2568117 and BankIt2568514.

AUTHOR CONTRIBUTIONS

KS, L-YL, and SG designed the research. KS, L-YL, JY, and SG performed the research. KS, L-YL, and SG analyzed the data. KS and SG wrote the manuscript with input from L-YL and JY. All authors contributed to the article and approved the submitted version.

FUNDING

This work was supported by a grant from the NSF (#1725122). We also wish to acknowledge support from the Purdue Center for Cancer Research *via* an NIH NCI grant (P30 CA023168), which supports the DNA Sequencing shared resources that were utilized in this work.

ACKNOWLEDGMENTS

The authors thank Ms. Laurel Jahn for help in T-circle isolation and characterization, and Ms. Neta Friedberg for help in constructing the T-circle binary vector pE4636. This work was

supported by a grant from the NSF (#1725122). We also wish to acknowledge support from the Purdue Center for Cancer Research *via* an NIH NCI grant (P30 CA023168), which supports the DNA Sequencing shared resources that were utilized in this work.

REFERENCES

- Bakkeren, G., Koukolikova-Nicola, Z., Girmsley, N., and Hohn, B. (1989).
 Recovery of Agrobacterium tumefaciens T-DNA molecules from whole plants early after transfer. Cell 57, 847–857. doi: 10.1016/0092-8674(89)90799-X
- Bravo-Angel, A. M., Hohn, B., and Tinland, B. (1998). The omega sequence of VirD2 is important but not essential for efficient transfer of T-DNA by Agrobacterium tumefaciens. Mol. Plant-Microbe Interact. 11, 57–63. doi: 10.1094/MPMI.1998.11.1.57
- Bundock, P., den Dulk-Ras, A., Beijersbergen, A., and Hooykaas, P. J. J. (1995).
 Trans-kingdom T-DNA transfer from Agrobacterium tumefaciens to Saccharomyces cerevisiae. EMBO J. 14, 3206–3214. doi: 10.1002/j.1460-2075.
 1995 tb07323 x
- Cascales, E., and Christie, P. J. (2004). Definition of a bacterial Type IV secretion pathway for a DNA substrate. Science 304, 1170–1173. doi: 10.1126/science. 1095211
- Castle, L. A., Errampalli, D., Atherton, T. L., Franzmann, L. H., Yoon, E. S., and Meinke, D. W. (1993). Genetic and molecular characterization of embryonic mutants identified following seed transformation in *Arabidopsis*. *Mol. Gen. Genet.* 241, 504–514. doi: 10.1007/BF00279892
- Clark, D. A., and Krysan, P. J. (2010). Chromosomal translocations are a common phenomenon in *Arabidopsis thaliana* T-DNA insertion lines. *Plant J.* 64, 990–1001. doi: 10.1111/j.1365-313X.2010.04386.x
- Curtis, M. J., Belcram, K., Bollmann, S. R., Tominey, C. M., Hoffman, P. D., Mercier, R., et al. (2009). Reciprocal chromosome translocation associated with T-DNA-insertion mutation in *Arabidopsis*: Genetic and cytological analyses of consequences for gametophyte development and for construction of doubly mutant lines. *Planta* 229, 731–745. doi: 10.1007/s00425-008-0868-0
- Durrenberger, F., Crameri, A., Hohn, B., and Koukolicova-Nicola, Z. (1989).
 Covalently bound VirD2 protein of Agrobacterium tumefaciens protects the T-DNA from exonucleolytic degradation. Proc. Natl. Acad. Sci. USA 86, 9154–9158. doi: 10.1073/pnas.86.23.9154
- Friesner, J., and Britt, A. B. (2003). *Ku80-* and *DNA ligase IV*-deficient plants are sensitive to ionizing radiation and defective in T-DNA integration. *Plant J.* 34, 427–440. doi: 10.1046/j.1365-313X.2003.01738.x
- Gallego, M. E., Bleuyard, J.-Y., Daoudal-Cotterell, S., Jallut, N., and White, C. I. (2003). Ku80 plays a role in non-homologous recombination but is not required for T-DNA integration in *Arabidopsis. Plant J.* 35, 557–565. doi: 10.1046/j.1365-313X.2003.01827.x
- Gelvin, S. B. (2010). Plant proteins involved in Agrobacterium-mediated genetic transformation. Annu. Rev. Phytopathol. 48, 45–68. doi: 10.1146/annurevphyto-080508-081852
- Gelvin, S. B. (2017). Integration of Agrobacterium T-DNA into the plant genome. Annu. Rev. Genet. 51, 195–217. doi: 10.1146/annurev-genet-120215-035320
- Gelvin, S. B. (2021). Plant DNA repair and Agrobacterium T-DNA integration. Internat. J. Mol. Sci. 22:8458. doi: 10.3390/ijms22168458
- Gorbunova, V., and Levy, A. A. (1997). Non-homologous DNA end joining in plant cells is associated with deletions and filler DNA insertions. *Nucl. Acids Res.* 25, 4650–4657. doi: 10.1093/nar/25.22.4650
- Hellens, R., Mullineaux, P., and Klee, H. (2000). A guide to Agrobacterium binary Ti vectors. Trends Plant Sci. 5, 446–451. doi: 10.1016/S1360-1385(00) 01740-4
- Hood, E. E., Gelvin, S. B., Melchers, L. S., and Hoekema, A. (1993). New Agrobacterium helper plasmids for gene transfer to plants. Transgen. Res. 2, 208–218. doi: 10.1007/BF01977351
- Howard, E., and Citovsky, V. (1990). The emerging structure of the Agrobacterium T-DNA transfer complex. BioEssays 12, 103–108. doi: 10.1002/bies.950120302
- Howard, E. A., Winsor, B. A., De Vos, G., and Zambryski, P. (1989). Activation of the T-DNA transfer process in *Agrobacterium* results in the generation of a T-strand-protein complex: tight association of VirD2 with the 5' ends

SUPPLEMENTARY MATERIAL

The Supplementary Material for this article can be found online at: https://www.frontiersin.org/articles/10.3389/fpls.2022.849930/full#supplementary-material

- of T-strands. Proc. Natl. Acad. Sci. USA 86, 4017-4021. doi: 10.1073/pnas.86.11.4017
- Hu, Y., Chen, Z., Zhung, C., and Huang, J. (2017). Cascade of chromosomal rearrangements caused by a heterogeneous T-DNA integration supports the double-strand break repair model for T-DNA integration. *Plant J.* 90, 954–965. doi: 10.1111/tpj.13523
- Jia, Q., Bundock, P., Hooykaas, P. J. J., and de Pater, S. (2012). Agrobacterium tumefaciens T-DNA integration and gene targeting in Arabidopsis thaliana non-homologous end-joining mutants. J. Bot. 2012;989272. doi: 10.1155/ 2012/989272
- Jupe, F., Rivkin, A. C., Michael, T. P., Zander, M., Motley, S. T., Sandoval, J. P., et al. (2019). The complex architecture and epigenomic impact of plant T-DNA insertions. *PLoS Genet*. 15:e1007819. doi: 10.1371/journal.pgen. 1007819
- Kent, T., Mateos-Gomez, P. A., Sfeir, A., and Pomerantz, R. T. (2016). Polymerase θ is a robust terminal transferase that oscillates between three different mechanisms during end-joining. eLIFE 5:e13740. doi: 10.7554/eLife.13740
- Kleinboelting, N., Huep, G., Appelhagen, I., Viehoever, P., Li, Y., and Weisshaar, B. (2015). The structural features of thousands of T-DNA insertion sites are consistent with a double-strand break repair based insertion mechanism. Mol. Plant 8, 1651–1664. doi: 10.1016/j.molp.2015.08.011
- Kononov, M. E., Bassuner, B., and Gelvin, S. B. (1997). Integration of T-DNA binary vector 'backbone' sequences into the tobacco genome: evidence for multiple complex patterns of integration. *Plant J.* 11, 945–957. doi: 10.1046/j. 1365-313X.1997.11050945.x
- Koukolikova-Nicola, Z., Shillito, R. D., Hohn, B., Wang, K., Van Montagu, M., and Zambryski, P. (1985). Involvement of circular intermediates in the transfer of T-DNA from Agrobacterium tumefaciens to plant cells. Nature 313, 191–196. doi: 10.1038/313191a0
- Lacroix, B., and Citovsky, V. (2019). Pathways of DNA transfer to plants from Agrobacterium tumefaciens and related bacterial species. Annu. Rev. Phytopathol. 57, 231–251. doi: 10.1146/annurev-phyto-082718-100101
- Lafleuriel, J., Degroote, F., Depeiges, A., and Picard, G. (2004). A reciprocal translocation, induced by a canonical integration of a single T-DNA, interrupts the HMG-I/Y Arabidopsis thaliana gene. Plant Physiol. Biochem. 42, 171–179. doi: 10.1016/j.plaphy.2004.01.003
- Li, J., Vaidya, M., White, C., Vainstein, A., Citovsky, V., and Tzfira, T. (2005). Involvement of Ku80 in T-DNA integration in plant cells. *Proc. Natl. Acad. Sci. USA* 102, 19231–19236. doi: 10.1073/pnas.0506437103
- Machida, Y., Usami, S., Yamamoto, A., Niwa, Y., and Takebe, I. (1986). Plant-inducible recombination between the 25 bp border sequences of T-DNA in Agrobacterium tumefaciens. Mol. Gen. Genet. 204, 374–382. doi: 10.1007/BF00331013
- Majhi, B. B., Shah, J. M., and Veluthambi, K. (2014). A novel T-DNA integration in rice involving two interchromosomal transloctions. *Plant Cell Rep.* 33, 929–944. doi: 10.1007/s00299-014-1572-0
- Mayerhofer, R., Koncz-Kalman, Z., Nawrath, C., Bakkeren, G., Cramer, A., Angelis, K., et al. (1991). T-DNA integration: A mode of illegitimate recombination in plants. *EMBO J.* 10, 697–704. doi: 10.1002/j.1460-2075.1991. tb07999.x
- Mestiri, I., Norre, F., Gallego, M. E., and White, C. I. (2014). Multiple host-cell recombination pathways act in *Agrobacterium*-mediated transformation of plant cells. *Plant J.* 77, 511–520. doi: 10.1111/tpj.12398
- Muller, A. E., Atkinson, R. G., Sandoval, R. B., and Jorgensen, R. A. (2007). Microhomologies between T-DNA ends and target sites often occur in inverted orientation and may be responsible for the high frequency of T-DNA-associated inversions. *Plant Cell Rep.* 26, 617–630. doi: 10.1007/s00299-006-0266-7
- Mysore, K. S., Bassuner, B., Deng, X. B., Darbinian, N. S., Motchoulski, A., Ream, W., et al. (1998). Role of the Agrobacterium tumefaciens VirD2 protein in T-DNA transfer and integration. Mol. Plant-Microbe Interact. 11, 668–683. doi: 10.1094/MPMI.1998.11.7.668

Nacry, P., Camilleri, C., Courtial, B., Caboche, M., and Bouchez, D. (1998). Major chromosomal rearrangements induced by T-DNA transformation in Arabidopsis. Genet. 149, 641–650. doi: 10.1093/genetics/149.2.641

- Narasimhulu, S. B., Deng, X.-B., Sarria, R., and Gelvin, S. B. (1996). Early transcription of Agrobacterium T-DNA genes in tobacco and maize. Plant Cell 8, 873–886. doi: 10.1105/tpc.8.5.873
- Nester, E. W. (2015). Agrobacterium: Nature's genetic engineer. Front. Plant Sci. 5:730. doi: 10.3389/fpls.2014.00730
- Nishizawa-Yokoi, A., Saika, H., Hara, N., Lee, L.-Y., Toki, S., and Gelvin, S. B. (2021). Agrobacterium T-DNA integration is somatic cells does not require the activity of DNA polymerase theta. New Phytol. 229, 2859–2872. doi: 10.1111/nph.17032
- Park, S.-Y., Vaghchhipawala, Z., Vasudevan, B., Lee, L.-Y., Shen, Y., Singer, K., et al. (2015). Agrobacterium T-DNA integration into the plant genome can occur without the activity of key non-homologous end-joining proteins. Plant J. 81, 934–946. doi: 10.1111/tpj.12779
- Rolloos, M., Dohmen, M. H. C., Hooykaas, P. J. J., and van der Zaal, B. (2014). Involvement of Rad52 in T-DNA circle formation during Agrobacterium tumefaciens-mediated transformation of Saccharomyces cerevisiae. Mol. Microbiol. 91, 1240–1251. doi: 10.1111/mmi.12531
- Rolloos, M., Hooykaas, P. J. J., and van der Zaal, B. (2015). Enhanced targeted integration mediated by translocated I-SceI during the Agrobacterium mediated transformation of yeast. Sci. Rep. 5:8345. doi: 10.1038/srep08345
- Rossi, L., Hohn, B., and Tinland, B. (1996). Integration of complete transferred DNA units is dependent on the activity of virulence E2 protein of Agrobacterium tumefaciens. Proc. Natl. Acad. Sci. USA 93, 126–130. doi: 10.1073/pnas.93.1.126
- Ruprecht, C., Carroll, A., and Persson, S. (2014). T-DNA-induced chromosomal translocation in *feronia* and *anxur2* mutants reveal implications for the mechanism of collapsed pollen due to chromosomal rearrangements. *Mol. Plant* 7, 1591–1594. doi: 10.1093/mp/ssu062
- Saika, H., Nishizawa-Yokoi, A., and Toki, S. (2014). The non-homologous endjoining pathway is involved in stable transformation in rice. Front. Plant Sci. 5:560. doi: 10.3389/fpls.2014.00560
- Schimmel, J., Kool, H., van Schendel, R., and Tijsterman, M. (2017). Mutational signatures of non-homologous and polymerase theta-mediated end-joining in embryonic stem cells. *EMBO J.* 36, 3634–3649. doi: 10.15252/ embj.201796948
- Shurvinton, C. E., Hodges, L., and Ream, W. (1992). A nuclear localization signal and the C-terminal omega sequence in the Agrobacterium tumefaciens VirD2 endonuclease are important for tumor formation. Proc. Natl. Acad. Sci. USA 89, 11837–11841. doi: 10.1073/pnas.89.24.11837
- Simpson, R. B., O'Hara, P. J., Kwok, W., Montoya, A. L., Lichtenstein, C., Gordon, M. P., et al. (1982). DNA from the A6S\2 crown gall tumor contains scrambled Ti-plasmid sequences near its junctions with plant DNA. *Cell* 29, 1005–1014. doi: 10.1016/0092-8674(82)90464-0
- Singer, K. (2018). "The mechanism of T-DNA integration: Some major unresolved questions" in Current Topics in Microbiology and Immunology: Agrobacterium Biology. From basic science to biotechnology, Vol. 148. ed. S. B. Gelvin (Cham: Springer), 287–317.
- Singer, K., Shiboleth, Y. M., Li, J., and Tzfira, T. (2012). Formation of complex extrachromosomal T- DNA structures in *Agrobacterium tumefaciens*-infected plants. *Plant Physiol.* 160, 511–522. doi: 10.1104/pp.112.200212
- Tax, F. E., and Vernon, D. M. (2001). T-DNA-associated duplication/translocations in *Arabidopsis*. Implications for mutant analysis and functional genomics. *Plant Physiol*. 126, 1527–1538. doi: 10.1104/pp.126.4.1527
- Tinland, B. (1996). The integration of T-DNA into plant genomes. *Trends Plant Sci.* 1, 178–184. doi: 10.1016/1360-1385(96)10020-0
- Tinland, B., and Hohn, B. (1995). "Recombination between prokaryotic and eukaryotic DNA: Integration of Agrobacterium tumefaciens T-DNA into the plant genome" in Genetic Engineering. ed. J. K. Setlow (New York: Plenum Press). 209–229.
- Tinland, B., Hohn, B., and Puchta, H. (1994). Agrobacterium tumefaciens transfers single-stranded transferred DNA (T-DNA) into the plant cell nucleus. Proc. Natl. Acad. Sci. USA 91, 8000-8004. doi: 10.1073/ pnas.91.17.8000
- Tinland, B., Schoumacher, F., Gloeckler, V., Bravo-Angel, A. M., and Hohn, B. (1995). The *Agrobacterium tumefaciens* virulence D2 protein is responsible for precise integration of T-DNA into the plant genome. *EMBO* J.14, 3585–3595.

- Tzfira, T., Li, J., Lacroix, B., and Citovsky, V. (2004). Agrobacterium T-DNA integration: Molecules and models. Trends Genet. 20, 375–383. doi: 10.1016/j. tig.2004.06.004
- Ulker, B., Li, Y., Rosso, M. G., Logemann, E., Somssich, I. E., and Weisshaar, B. (2008). T-DNA-mediated transfer of Agrobacterium tumefaciens chromosomal DNA into plants. Nature Biotechnol. 26, 1015–1017. doi: 10.1038/nbt.1491
- Vaghchhipawala, Z. E., Vasudevan, B., Lee, S., Morsy, M. R., and Mysore, K. S. (2012). Agrobacterium may delay plant nonhomologous end-joining DNA repair via XRCC4 to favor T-DNA integration. Plant Cell 24, 4110–4123. doi: 10.1105/tpc.112.100495
- van Attikum, H., Bundock, P., Lee, L.-Y., Gelvin, S. B., and Hooykaas, P. J. J. (2003). The Arabidopsis AtLIG4 gene is involved in the repair of DNA damage, but not in the integration of *Agrobacterium T-DNA*. *Nucl. Acids Res.* 4255, 4247–4123. doi: 10.1093/nar/gkg458
- van Kregten, M., de Pater, S., Romeijn, R., van Schendel, R., Hooykaas, P. J. J., and Tijsterman, M. (2016). T-DNA integration in plants results from polymerase-theta-mediated DNA repair. *Nature Plants* 2:16164. doi: 10.1038/nplants.2016.164
- van Kregten, M., Lindhout, B. I., Hooykaas, P. J. J., and van der Zaal, B. J. (2009). Agrobacterium-mediated T-DNA transfer and integration by minimal VirD2 consisting of the relaxase domain and a type IV secretion system translocation signal. Mol. Plant-Microbe Interact. 22, 1356–1365. doi: 10.1094/MPMI-22-11-1356
- Wang, K., Stachel, S. E., Timmerman, B., Van Montagu, M., and Zambryski, P. C. (1987). Site-specific nick in the T-DNA border sequence as a result of Agrobacterium vir gene expression. Science 235, 587–591. doi: 10.1126/ science.235.4788.587
- Ward, E. R., and Barnes, W. M. (1988). VirD2 protein of Agrobacterium tumefaciens very tightly linked to the 5' end of T-strand DNA. Science 242, 927–930. doi: 10.1126/science.242.4880.927
- Wenck, A., Czako, M., Kanevski, I., and Marton, L. (1997). Frequent collinear long transfer of DNA inclusive of the whole binary vector during *Agrobacterium*mediated transformation. *Plant Mol. Biol.* 34, 913–922. doi: 10.1023/ A:1005849303333
- Windels, P., De Buck, S., Van Bockstaele, E., De Loose, M., and Depicker, A. (2003). T-DNA integration in *Arabidopsis* chromosomes. Presence and origin of filler DNA sequences. *Plant Physiol*. 133, 2061–2068. doi: 10.1104/pp.103.027532
- Wu, H.-Y., Liu, K.-H., Wang, Y.-C., Wu, J.-F., Chiu, W.-L., Chen, C.-Y., et al. (2014). AGROBEST: an efficient Agrobacterium-mediated transient expression method for versatile gene function analyses in Arabidopsis seedlings. Plant Meth. 10:19. doi: 10.1186/1746-4811-10-19
- Wyatt, D. W., Feng, W., Conlin, M. P., Yousefzadeh, M. J., Robers, S. A., Mieczdowski, P., et al. (2016). Essential roles for polymerase θ-mediated end joining in the repair of chromosome breaks. *Mol. Cell* 63, 662–673. doi: 10.1016/j.molcel.2016.06.020
- Young, C., and Nester, E. W. (1988). Association of the VirD2 protein with the 5' end of T strands in *Agrobacterium tumefaciens*. *J. Bacteriol*. 170, 3367–3374. doi: 10.1128/jb.170.8.3367-3374.1988
- Yusibov, V. M., Steck, T. R., Gupta, V., and Gelvin, S. B. (1994). Association of single-stranded transferred DNA from *Agrobacterium tumefaciens* with tobacco cells. *Proc. Natl. Acad. Sci. USA* 91, 2994–2998. doi: 10.1073/pnas.91.8.2994
- Zhang, Y., Chen, M., Siemiatkowska, B., Toleco, M. R., Jing, Y., Strotmann, V., et al. (2020). A highly efficient *Agrobacterium*-mediated method for transient gene expression and functional studies in multiple plant species. *Plant Commun.* 1:100028. doi: 10.1016/j.xplc.2020.100028
- Zipfel, C., Kunze, G., Chinchilla, D., Caniard, A., Jones, J. D. G., Boller, T., et al. (2006). Perception of the bacterial PAMP EF-Tu by the receptor EFR restricts Agrobacterium-mediated transformation. Cell 125, 749–760. doi: 10.1016/j.cell.2006.03.037
- **Conflict of Interest:** The authors declare that the research was conducted in the absence of any commercial or financial relationships that could be construed as a potential conflict of interest.
- **Publisher's Note:** All claims expressed in this article are solely those of the authors and do not necessarily represent those of their affiliated organizations, or those of the publisher, the editors and the reviewers. Any product that may

be evaluated in this article, or claim that may be made by its manufacturer, is not guaranteed or endorsed by the publisher.

Copyright © 2022 Singer, Lee, Yuan and Gelvin. This is an open-access article distributed under the terms of the Creative Commons Attribution License

(CC BY). The use, distribution or reproduction in other forums is permitted, provided the original author(s) and the copyright owner(s) are credited and that the original publication in this journal is cited, in accordance with accepted academic practice. No use, distribution or reproduction is permitted which does not comply with these terms.

No.	Sample No.	Strain	Construct	Monomeric/Complex*
N. benthai	miana with TET-OF	RI:		
1	#001-1	EHA105	TET-ORI	complex
2	#001-2	EHA105	TET-ORI	monomeric
3	#001-4	EHA105	TET-ORI	monomeric
4	#001-5	EHA105	TET-ORI	monomeric
5	#001-6	EHA105	TET-ORI	monomeric
6	#002-19	EHA105	TET-ORI	monomeric
7	#002-20	EHA105	TET-ORI	complex
8	#002-21	EHA105	TET-ORI	complex
9	#002-22	EHA105	TET-ORI	monomeric
10	#002-23	EHA105	TET-ORI	complex
11	#002-25	EHA105	TET-ORI	monomeric
12	#002-26	EHA105	TET-ORI	monomeric
13	#003-50	EHA105	TET-ORI	complex
14	#003-51	EHA105	TET-ORI	complex
15	#003-52	EHA105	TET-ORI	monomeric
16	#003-53	EHA105	TET-ORI	monomeric
17	#003-54	EHA105	TET-ORI	complex
18	#003-55	EHA105	TET-ORI	monomeric
19	#003-56	EHA105	TET-ORI	monomeric
20	#003-57	EHA105	TET-ORI	monomeric
21	#003-58	EHA105	TET-ORI	monomeric
22	#003-59	EHA105	TET-ORI	monomeric
23	#003-60	EHA105	TET-ORI	complex
24	#003-61	EHA105	TET-ORI	complex
25	#003-62	EHA105	TET-ORI	complex
26	#003-63	EHA105	TET-ORI	monomeric
27	#003-64	EHA105	TET-ORI	complex
28	#003-65	EHA105	TET-ORI	monomeric
29	#003-66	EHA105	TET-ORI	monomeric
30	#003-67	EHA105	TET-ORI	monomeric
31	#003-68	EHA105	TET-ORI	complex
32	#003-69	EHA105	TET-ORI	monomeric
33	#003-70	EHA105	TET-ORI	monomeric
34	#008-49	EHA105	TET-ORI	complex
35	#008-50	EHA105	TET-ORI	complex
36	#008-51	EHA105	TET-ORI	complex
37	#008-52	EHA105	TET-ORI	monomeric
38	#008-53	EHA105	TET-ORI	complex
39	#008-54	EHA105	TET-ORI	monomeric
40	#008-55	EHA105	TET-ORI	monomeric
41	#008-57	EHA105	TET-ORI	monomeric
42	#008-58	EHA105	TET-ORI	monomeric
43	#008-59	EHA105	TET-ORI	monomeric
44	#008-60	EHA105	TET-ORI	complex
45	#008-61	EHA105	TET-ORI	complex

46	#008-62	EHA105	TET-ORI	complex
47	#008-63	EHA105	TET-ORI	complex
48	#008-64	EHA105	TET-ORI	monomeric
49	#008-65	EHA105	TET-ORI	monomeric
50	#008-66	EHA105	TET-ORI	complex
51	#008-67	EHA105	TET-ORI	monomeric
52	#008-68	EHA105	TET-ORI	monomeric
53	#008-69	EHA105	TET-ORI	monomeric
54	#008-70	EHA105	TET-ORI	monomeric
55	#008-71	EHA105	TET-ORI	monomeric
56	#008-72	EHA105	TET-ORI	monomeric
57	#008-73	EHA105	TET-ORI	complex
58	#008-74	EHA105	TET-ORI	monomeric
59	#008-75	EHA105	TET-ORI	monomeric
60	#008-76	EHA105	TET-ORI	complex
61	#008-77	EHA105	TET-ORI	complex
62	#008-78	EHA105	TET-ORI	monomeric
63	#008-79	EHA105	TET-ORI	complex
64	#008-80	EHA105	TET-ORI	complex
65	#008-81	EHA105	TET-ORI	monomeric
66	#008-82	EHA105	TET-ORI	monomeric
67	#008-83	EHA105	TET-ORI	complex
68	#008-84	EHA105	TET-ORI	complex
69	#008-85	EHA105	TET-ORI	complex
70	#008-86	EHA105	TET-ORI	complex
71	#008-87	EHA105	TET-ORI	monomeric
72	#008-88	EHA105	TET-ORI	complex
73	#008-89	EHA105	TET-ORI	monomeric
74	#008-90	EHA105	TET-ORI	complex
75	#009-1	EHA105	TET-ORI	complex
76	#009-2	EHA105	TET-ORI	monomeric
77	#009-3	EHA105	TET-ORI	monomeric
78	#009-4	EHA105	TET-ORI	monomeric
79	#009-5	EHA105	TET-ORI	complex
80	#009-10	EHA105	TET-ORI	complex
81	#009-11	EHA105	TET-ORI	monomeric
82	#009-12	EHA105	TET-ORI	complex
83	#009-13	EHA105	TET-ORI	monomeric
84	#009-14	EHA105	TET-ORI	complex
85	#009-15	EHA105	TET-ORI	monomeric
86	#009-16	EHA105	TET-ORI	monomeric
87	#009-17	EHA105	TET-ORI	monomeric
88	#009-18	EHA105	TET-ORI	monomeric
89	#009-19	EHA105	TET-ORI	monomeric
90	#009-21	EHA106	TET-ORI	monomeric
91	#009-22	EHA105	TET-ORI	complex
92	#009-23	EHA105	TET-ORI	monomeric
93	#009-24	EHA105	TET-ORI	monomeric

94	#009-25	EHA105	TET-ORI	monomeric
95	#009-26	EHA105	TET-ORI	monomeric
96	#009-27	EHA105	TET-ORI	monomeric
97	#009-28	EHA105	TET-ORI	monomeric
98	#011-29	EHA105	TET-ORI	complex
99	#011-30	EHA105	TET-ORI	monomeric
100	#011-31	EHA105	TET-ORI	complex
101	#011-32	EHA105	TET-ORI	complex
102	#011-33	EHA105	TET-ORI	complex
103	#011-34	EHA105	TET-ORI	monomeric
104	#011-35	EHA105	TET-ORI	monomeric
105	#011-36	EHA105	TET-ORI	monomeric
106	#011-37	EHA105	TET-ORI	monomeric
107	#011-38	EHA105	TET-ORI	monomeric

N. benthamiana with AMP-ORI:

1	#050-1	EHA105	AMP-ORI	monomeric
2	#050-2	EHA105	AMP-ORI	monomeric
3	#050-3	EHA105	AMP-ORI	monomeric
4	#050-4	EHA105	AMP-ORI	monomeric
5	#050-5	EHA105	AMP-ORI	monomeric
6	#050-6	EHA105	AMP-ORI	monomeric
7	#050-7	EHA105	AMP-ORI	complex
8	#050-8	EHA105	AMP-ORI	complex
9	#050-9	EHA105	AMP-ORI	monomeric
10	#050-10	EHA105	AMP-ORI	monomeric
11	#050-11	EHA105	AMP-ORI	monomeric
12	#050-12	EHA105	AMP-ORI	complex
13	#050-13	EHA105	AMP-ORI	complex
14	#050-14	EHA105	AMP-ORI	complex
15	#050-15	EHA105	AMP-ORI	monomeric
16	#050-16	EHA105	AMP-ORI	monomeric
17	#050-17	EHA105	AMP-ORI	complex
18	#050-18	EHA105	AMP-ORI	monomeric
19	#050-19	EHA105	AMP-ORI	monomeric
20	#050-21	EHA105	AMP-ORI	monomeric
21	#050-22	EHA105	AMP-ORI	complex
22	#050-23	EHA105	AMP-ORI	complex
23	#050-24	EHA105	AMP-ORI	monomeric
24	#050-25	EHA105	AMP-ORI	monomeric
25	#050-26	EHA105	AMP-ORI	monomeric
26	#050-27	EHA105	AMP-ORI	monomeric
27	#050-28	EHA105	AMP-ORI	monomeric
28	#050-29	EHA105	AMP-ORI	complex
29	#050-30	EHA105	AMP-ORI	monomeric
30	#050-31	EHA105	AMP-ORI	complex
31	#050-33	EHA105	AMP-ORI	monomeric
32	#050-34	EHA105	AMP-ORI	monomeric

33	#050-35	EHA105	AMP-ORI	monomeric
34	#050-36	EHA105	AMP-ORI	monomeric
35	#050-37	EHA105	AMP-ORI	monomeric
36	#050-38	EHA105	AMP-ORI	monomeric
37	#050-39	EHA105	AMP-ORI	monomeric
38	#050-40	EHA105	AMP-ORI	monomeric
39	#052-1	EHA105	AMP-ORI	complex
40	#052-2	EHA105	AMP-ORI	complex
41	#052-3	EHA105	AMP-ORI	monomeric
42	#052-4	EHA105	AMP-ORI	monomeric
43	#052-5	EHA105	AMP-ORI	monomeric
44	#052-6	EHA105	AMP-ORI	monomeric
45	#052-7	EHA105	AMP-ORI	monomeric
46	#052-8	EHA105	AMP-ORI	monomeric
47	#052-9	EHA105	AMP-ORI	complex
48	#052-10	EHA105	AMP-ORI	monomeric
49	#052-11	EHA105	AMP-ORI	monomeric
50	#052-12	EHA105	AMP-ORI	complex
51	#052-13	EHA105	AMP-ORI	monomeric
52	#052-14	EHA105	AMP-ORI	monomeric
53	#052-15	EHA105	AMP-ORI	monomeric
54	#052-16	EHA105	AMP-ORI	monomeric
55	#052-17	EHA105	AMP-ORI	complex
56	#052-18	EHA105	AMP-ORI	complex
57	#052-19	EHA105	AMP-ORI	monomeric
58	#052-20	EHA105	AMP-ORI	monomeric
59	#052-21	EHA105	AMP-ORI	complex
60	#052-22	EHA105	AMP-ORI	complex
61	#052-23	EHA105	AMP-ORI	monomeric
62	#052-24	EHA105	AMP-ORI	monomeric
63	#052-25	EHA105	AMP-ORI	complex
64	#052-26	EHA105	AMP-ORI	monomeric
65	#052-27	EHA105	AMP-ORI	complex
66	#052-28	EHA105	AMP-ORI	complex
67	#052-29	EHA105	AMP-ORI	monomeric
68	#052-30	EHA105	AMP-ORI	monomeric
69	#052-31	EHA105	AMP-ORI	monomeric
70	#052-32	EHA105	AMP-ORI	complex
71	#052-33	EHA105	AMP-ORI	monomeric
72	#052-34	EHA105	AMP-ORI	complex
73	#052-35	EHA105	AMP-ORI	complex
74	#052-36	EHA105	AMP-ORI	monomeric
75	#052-37	EHA105	AMP-ORI	monomeric
76	#052-38	EHA105	AMP-ORI	monomeric
77	#052-40	EHA105	AMP-ORI	monomeric
78	#052-41	EHA105	AMP-ORI	monomeric
79	#052-42	EHA105	AMP-ORI	complex
80	#052-43	EHA105	AMP-ORI	monomeric

81	#052-44	EHA105	AMP-ORI	complex
82	#052-45	EHA105	AMP-ORI	complex
83	#052-46	EHA105	AMP-ORI	monomeric
84	#052-48	EHA105	AMP-ORI	monomeric
85	#052-49	EHA105	AMP-ORI	monomeric
86	#052-50	EHA105	AMP-ORI	monomeric
87	#052-51	EHA105	AMP-ORI	monomeric
88	#052-52	EHA105	AMP-ORI	monomeric
89	#052-53	EHA105	AMP-ORI	complex
90	#052-54	EHA105	AMP-ORI	monomeric
91	#052-55	EHA105	AMP-ORI	complex
92	#052-56	EHA105	AMP-ORI	monomeric
93	#052-57	EHA105	AMP-ORI	monomeric
94	#052-58	EHA105	AMP-ORI	monomeric
95	#052-59	EHA105	AMP-ORI	monomeric
96	#052-60	EHA105	AMP-ORI	complex
97	#052-61	EHA105	AMP-ORI	monomeric
98	#052-62	EHA105	AMP-ORI	monomeric
99	#052-63	EHA105	AMP-ORI	complex
100	#052-64	EHA105	AMP-ORI	monomeric
101	#052-65	EHA105	AMP-ORI	monomeric
102	#052-66	EHA105	AMP-ORI	complex
103	#052-67	EHA105	AMP-ORI	monomeric
104	#052-68	EHA105	AMP-ORI	complex
N. benthamia	na with $VirD2Ω$:			•
1	#005-1	At1959	TET-ORI	monomeric
2	#005-2	At1959	TET-ORI	monomeric
3	#005-3	At1959	TET-ORI	monomeric
4	#005-4	At1959	TET-ORI	complex
5	#005-6	At1959	TET-ORI	complex
6	#005-7	At1959	TET-ORI	monomeric
7	#005-8	At1959	TET-ORI	complex
8	#005-9	At1959	TET-ORI	monomeric
9	#055-1	At1959	AMP-ORI	monomeric
10	#055-2	At1959	AMP-ORI	monomeric
Arabidopsis (Col-0			
1	#021-1	EHA105	AMP-ORI	monomeric
2	#021-2	EHA105	AMP-ORI	monomeric
3	#021-3	EHA105	AMP-ORI	complex
4	#021-4	EHA105	AMP-ORI	complex
5	#021-5	EHA105	AMP-ORI	monomeric
6	#021-6	EHA105	AMP-ORI	monomeric
7	#021-7	EHA105	AMP-ORI	monomeric
8	#021-8	EHA105	AMP-ORI	monomeric
9	#021-9	EHA105	AMP-ORI	monomeric
10	#021-10	EHA105	AMP-ORI	monomeric
11	#021-11	EHA105	AMP-ORI	monomeric
12	#021-12	EHA105	AMP-ORI	monomeric

13	#021-13	EHA105	AMP-ORI	monomeric
Arabidopsis	s efr-1			
1	#022-1	EHA105	AMP-ORI	monomeric
2	#022-2	EHA105	AMP-ORI	monomeric
3	#022-3	EHA105	AMP-ORI	monomeric
4	#022-4	EHA105	AMP-ORI	monomeric
5	#022-5	EHA105	AMP-ORI	monomeric
6	#022-6	EHA105	AMP-ORI	monomeric
7	#022-7	EHA105	AMP-ORI	monomeric
8	#022-8	EHA105	AMP-ORI	monomeric
9	#022-9	EHA105	AMP-ORI	monomeric
10	#022-10	EHA105	AMP-ORI	monomeric
11	#022-11	EHA105	AMP-ORI	monomeric
12	#022-12	EHA105	AMP-ORI	monomeric
13	#022-13	EHA105	AMP-ORI	monomeric
14	#022-14	EHA105	AMP-ORI	monomeric
15	#022-15	EHA105	AMP-ORI	monomeric
16	#022-16	EHA105	AMP-ORI	monomeric
17	#022-17	EHA105	AMP-ORI	monomeric
18	#022-18	EHA105	AMP-ORI	monomeric
19	#022-19	EHA105	AMP-ORI	monomeric
20	#022-20	EHA105	AMP-ORI	monomeric
21	#022-21	EHA105	AMP-ORI	monomeric
22	#022-22	EHA105	AMP-ORI	monomeric
23	#022-23	EHA105	AMP-ORI	monomeric
24	#022-24	EHA105	AMP-ORI	monomeric
25	#022-25	EHA105	AMP-ORI	monomeric
26	#022-26	EHA105	AMP-ORI	monomeric
27	#022-27	EHA105	AMP-ORI	monomeric
28	#022-28	EHA105	AMP-ORI	monomeric
29	#022-29	EHA105	AMP-ORI	monomeric
30	#022-30	EHA105	AMP-ORI	monomeric
31	#022-31	EHA105	AMP-ORI	monomeric
32	#022-32	EHA105	AMP-ORI	monomeric
33	#022-33	EHA105	AMP-ORI	monomeric
34	#022-34	EHA105	AMP-ORI	monomeric
35	#022-35	EHA105	AMP-ORI	monomeric
36	#022-36	EHA105	AMP-ORI	monomeric
37	#022-37	EHA105	AMP-ORI	monomeric
38	#022-38	EHA105	AMP-ORI	monomeric
39	#022-39	EHA105	AMP-ORI	monomeric
40	#022-40	EHA105	AMP-ORI	monomeric
41	#022-41	EHA105	AMP-ORI	monomeric
42	#022-42	EHA105	AMP-ORI	monomeric
43	#022-43	EHA105	AMP-ORI	monomeric
44	#022-44	EHA105	AMP-ORI	monomeric
45	#022-45	EHA105	AMP-ORI	monomeric

46	#022-46	EHA105	AMP-ORI	monomeric
47	#022-47	EHA105	AMP-ORI	monomeric
48	#022-48	EHA105	AMP-ORI	monomeric
49	#025-49	EHA105	AMP-ORI	monomeric
50	#046-1	EHA105	AMP-ORI	monomeric
51	#046-2	EHA105	AMP-ORI	monomeric
52	#046-3	EHA105	AMP-ORI	monomeric
53	#046-4	EHA105	AMP-ORI	monomeric
54	#046-5	EHA105	AMP-ORI	monomeric
55	#046-6	EHA105	AMP-ORI	monomeric
56	#046-7	EHA105	AMP-ORI	monomeric
57	#046-8	EHA105	AMP-ORI	monomeric
58	#046-9	EHA105	AMP-ORI	monomeric
59	#046-10	EHA105	AMP-ORI	monomeric
60	#046-11	EHA105	AMP-ORI	monomeric
61	#046-12	EHA105	AMP-ORI	monomeric
62	#046-13	EHA105	AMP-ORI	monomeric
63	#046-14	EHA105	AMP-ORI	monomeric
64	#046-15	EHA105	AMP-ORI	monomeric
65	#046-16	EHA105	AMP-ORI	monomeric
66	#046-17	EHA105	AMP-ORI	monomeric
67	#046-18	EHA105	AMP-ORI	monomeric
68	#046-19	EHA105	AMP-ORI	monomeric
69	#046-20	EHA105	AMP-ORI	monomeric
70	#046-21	EHA105	AMP-ORI	complex
71	#046-22	EHA105	AMP-ORI	monomeric
72	#046-23	EHA105	AMP-ORI	monomeric
73	#046-24	EHA105	AMP-ORI	monomeric
74	#046-25	EHA105	AMP-ORI	monomeric
75	#046-26	EHA105	AMP-ORI	monomeric
76	#046-27	EHA105	AMP-ORI	
77	#046-28	EHA105	AMP-ORI	monomeric
78	#046-29	EHA105	AMP-ORI	monomeric
79	#046-30	EHA105	AMP-ORI	monomeric
80	#046-31	EHA105	AMP-ORI	monomeric
81	#046-32	EHA105	AMP-ORI	monomeric
82	#046-33	EHA105	AMP-ORI	monomeric
83	#046-34	EHA105	AMP-ORI	monomeric
84	#046-35	EHA105	AMP-ORI	monomeric
85	#046-36	EHA105	AMP-ORI	monomeric
86	#046-37	EHA105	AMP-ORI	monomeric
87	#046-38	EHA105	AMP-ORI	monomeric
88	#046-39	EHA105	AMP-ORI	monomeric
89	#046-40	EHA105	AMP-ORI	monomeric
90	#046-40 #046-41	EHA105	AMP-ORI	monomeric
91	#046-41 #046-42	EHA105	AMP-ORI	monomeric
91	#046-42 #046-43	EHA105	AMP-ORI	monomeric
93	#046-44 #046-44	EHA105	AMP-ORI	
93	#U 1 U-44	ЕПАТОЭ	AWIF-UKI	monomeric

94	#046-45	EHA105	AMP-ORI	monomeric
95	#046-46	EHA105	AMP-ORI	monomeric
96	#046-47	EHA105	AMP-ORI	monomeric
97	#046-48	EHA105	AMP-ORI	monomeric
98	#046-49	EHA105	AMP-ORI	monomeric
99	#047-1	EHA105	AMP-ORI	monomeric
100	#047-2	EHA105	AMP-ORI	monomeric
101	#047-3	EHA105	AMP-ORI	complex
102	#047-4	EHA105	AMP-ORI	monomeric
103	#047-5	EHA105	AMP-ORI	monomeric
104	#047-6	EHA105	AMP-ORI	monomeric
105	#047-7	EHA105	AMP-ORI	monomeric
106	#047-8	EHA105	AMP-ORI	monomeric
107	#047-9	EHA105	AMP-ORI	monomeric
108	#047-11	EHA105	AMP-ORI	monomeric
109	#047-12	EHA105	AMP-ORI	monomeric
110	#047-13	EHA105	AMP-ORI	monomeric
111	#047-14	EHA105	AMP-ORI	monomeric
112	#047-15	EHA105	AMP-ORI	monomeric
113	#047-16	EHA105	AMP-ORI	monomeric
114	#047-17	EHA105	AMP-ORI	monomeric
115	#047-18	EHA105	AMP-ORI	monomeric
116	#047-19	EHA105	AMP-ORI	monomeric
117	#047-20	EHA105	AMP-ORI	monomeric
118	#047-21	EHA105	AMP-ORI	monomeric
119	#047-22	EHA105	AMP-ORI	monomeric
120	#047-23	EHA105	AMP-ORI	monomeric
121	#041-1	EHA105	AMP-ORI	monomeric
122	#041-2	EHA105	AMP-ORI	monomeric
123	#041-3	EHA105	AMP-ORI	monomeric
124	#041-4	EHA105	AMP-ORI	monomeric
125	#041-5	EHA105	AMP-ORI	monomeric
126	#041-6	EHA105	AMP-ORI	monomeric
127	#041-7	EHA105	AMP-ORI	monomeric
128	#041-8	EHA105	AMP-ORI	monomeric
129	#041-9	EHA105	AMP-ORI	monomeric
130	#041-10	EHA105	AMP-ORI	monomeric
Arabidopsis	efr-1/ku80			
1	#043-1	EHA105	AMP-ORI	monomeric
2	#043-2	EHA105	AMP-ORI	monomeric
3	#043-3	EHA105	AMP-ORI	monomeric
4	#043-4	EHA105	AMP-ORI	monomeric
5	#043-5	EHA105	AMP-ORI	monomeric
6	#043-6	EHA105	AMP-ORI	monomeric
7	#043-7	EHA105	AMP-ORI	monomeric
8	#043-8	EHA105	AMP-ORI	monomeric
9	#043-9	EHA105	AMP-ORI	monomeric
-	,, , , ,	21111100	0101	

10	#043-10	EHA105	AMP-ORI	monomeric
11	#043-11	EHA105	AMP-ORI	monomeric
12	#043-12	EHA105	AMP-ORI	monomeric
13	#043-15	EHA105	AMP-ORI	monomeric
14	#043-16	EHA105	AMP-ORI	monomeric
15	#043-17	EHA105	AMP-ORI	monomeric
16	#043-18	EHA105	AMP-ORI	monomeric
17	#043-19	EHA105	AMP-ORI	monomeric
18	#043-20	EHA105	AMP-ORI	monomeric
19	#043-21	EHA105	AMP-ORI	monomeric
20	#043-22	EHA105	AMP-ORI	monomeric
21	#043-23	EHA105	AMP-ORI	monomeric
22	#043-24	EHA105	AMP-ORI	monomeric
23	#043-25	EHA105	AMP-ORI	complex
24	#043-26	EHA105	AMP-ORI	monomeric
25	#043-27	EHA105	AMP-ORI	monomeric
26	#043-28	EHA105	AMP-ORI	monomeric
27	#043-29	EHA105	AMP-ORI	monomeric
28	#043-30	EHA105	AMP-ORI	complex
29	#043-31	EHA105	AMP-ORI	monomeric
30	#043-32	EHA105	AMP-ORI	monomeric
31	#043-33	EHA105	AMP-ORI	monomeric
32	#043-34	EHA105	AMP-ORI	monomeric
33	#043-35	EHA105	AMP-ORI	monomeric
34	#043-36	EHA105	AMP-ORI	monomeric
35	#043-37	EHA105	AMP-ORI	monomeric
36	#043-38	EHA105	AMP-ORI	monomeric
37	#043-39	EHA105	AMP-ORI	monomeric
38	#043-40	EHA105	AMP-ORI	monomeric
39	#043-41	EHA105	AMP-ORI	complex
40	#043-42	EHA105	AMP-ORI	monomeric
41	#043-43	EHA105	AMP-ORI	monomeric
42	#043-44	EHA105	AMP-ORI	monomeric
43	#043-45	EHA105	AMP-ORI	monomeric
44	#043-46	EHA105	AMP-ORI	monomeric
45	#043-47	EHA105	AMP-ORI	monomeric
46	#045-1	EHA105	AMP-ORI	monomeric
47	#045-2	EHA105	AMP-ORI	monomeric
48	#045-3	EHA105	AMP-ORI	monomeric
49	#045-4	EHA105	AMP-ORI	monomeric
50	#045-5	EHA105	AMP-ORI	monomeric
51	#045-6	EHA105	AMP-ORI	monomeric
52	#045-7	EHA105	AMP-ORI	monomeric
53	#045-8	EHA105	AMP-ORI	monomeric
54	#045-9	EHA105	AMP-ORI	monomeric
55	#045-10	EHA105	AMP-ORI	monomeric
56	#045-11	EHA105	AMP-ORI	monomeric
57	#045-12	EHA105	AMP-ORI	monomeric

58	#045-13	EHA105	AMP-ORI	complex
59	#045-14	EHA105	AMP-ORI	monomeric
60	#045-15	EHA105	AMP-ORI	monomeric
61	#045-16	EHA105	AMP-ORI	monomeric
62	#045-17	EHA105	AMP-ORI	monomeric
63	#045-18	EHA105	AMP-ORI	monomeric
64	#045-19	EHA105	AMP-ORI	monomeric
65	#045-20	EHA105	AMP-ORI	monomeric
66	#045-21	EHA105	AMP-ORI	monomeric
67	#045-22	EHA105	AMP-ORI	monomeric
68	#045-23	EHA105	AMP-ORI	monomeric
69	#045-24	EHA105	AMP-ORI	monomeric
70	#045-25	EHA105	AMP-ORI	monomeric
71	#045-26	EHA105	AMP-ORI	monomeric
72	#045-27	EHA105	AMP-ORI	monomeric
73	#045-28	EHA105	AMP-ORI	monomeric
74	#045-29	EHA105	AMP-ORI	monomeric
75	#045-30	EHA105	AMP-ORI	monomeric

^{*} Determination of monomeric or complex structure was done by agarose gel analysis. When result was uncertain T-circles were further sequenced and classified accordingly.

Supplemental Table 2. Sequenced T-DNA junctions of monomeric T-circles from N. benthamiana

	1 Table 2. Se	equenced T-D	NA junctions of mo	onomeric T-circles fr		ana
Sample	Q		p.p.a		Filler	ı Dâ
No.	Strain	Construct	RB ^a	Microhomology	DNA	LB ^a
#001-2	EHA105	TET-ORI	precise	0	1 (T)	-25
#001-2 #001-4	EHA105	TET-ORI	precise	0	0	-2 <i>3</i> -11
#001-5	EHA105	TET-ORI	-2	2 (TT)	0	-32
#001-6	EHA105	TET-ORI	precise	12 ^b	0	precise
#002-19	EHA105	TET-ORI	precise	12 ^b	0	precise
#002-22	EHA105	TET-ORI	precise	12 ^b	0	precise
#002-25	EHA105	TET-ORI	precise	0	0	-82
#002-26	EHA105	TET-ORI	precise	12 ^b	0	precise
#003-52	EHA105	TET-ORI	precise	12 ^b	0	precise
#003-53	EHA105	TET-ORI	precise	12 ^b	0	precise
#003-55	EHA105	TET-ORI	precise + 2 ^c	2 (CA)	0	-98
#003-56	EHA105	TET-ORI	precise	0	1 (T)	-23
#003-57	EHA105	TET-ORI	precise	12 ^b	0	precise
#003-58	EHA105	TET-ORI	-1	3 (TTG)	0	-52
#003-59	EHA105	TET-ORI	precise	12 ^b	0	precise
#003-63	EHA105	TET-ORI	precise	12 ^b	0	precise
#003-65	EHA105	TET-ORI	precise	0	0	-65
#003-66	EHA105	TET-ORI	precise	12 ^b	0	precise
#003-67	EHA105	TET-ORI	precise	12 ^b	0	precise
#003-70	EHA105	TET-ORI	precise	12 ^b	0	precise
#008-55	EHA105	TET-ORI	precise	12 ^b	0	precise
#008-57	EHA105	TET-ORI	-2	0	1 (A)	-27
#008-59	EHA105	TET-ORI	precise	12 ^b	0	precise
#008-67	EHA105	TET-ORI	precise	12 ^b	0	precise
#008-68	EHA105	TET-ORI	precise	12 ^b	0	precise
#008-69	EHA105	TET-ORI	precise + 2 bp ^c	2 (CA)	0	-1
#008-71	EHA105	TET-ORI	precise	12 ^b	0	precise
#008-72	EHA105	TET-ORI	precise	0	1 (A)	-69
#008-75	EHA105	TET-ORI	precise	0	1 (A)	-8
#008-82	EHA105	TET-ORI	precise	12 ^b	0	precise
#009-2	EHA105	TET-ORI	-3	0	0	-71
#009-3	EHA105	TET-ORI	precise	0	4 (AAAA)	-175
#009-4	EHA105	TET-ORI	precise	12 ^b	0	precise
#009-11	EHA105	TET-ORI	precise	12 ^b	0	precise
#009-13	EHA105	TET-ORI	precise	0	0	-22
#009-17	EHA105	TET-ORI	precise	12 ^b	0	precise
#009-18	EHA105	TET-ORI	precise	12 ^b	0	precise
#009-19	EHA105	TET-ORI	precise	12 ^b	0	precise

//000 21	FILA 106	TET ON		0	1 (T)	06
#009-21	EHA106	TET-ORI	precise	0	1 (T)	-96
#009-26	EHA105	TET-ORI	precise	0 0	0	-70
#011-30	EHA105	TET-ORI	-16		0	-16
#011-34	EHA105	TET-ORI	precise	12 ^b	0	precise
#011-35	EHA105	TET-ORI	precise + 7 bp	10	0	-100
#011 26	EHA 105	TET-ORI	m maaiga	(TGTTTGACAG) 0	0	-62
#011-36 #011-38	EHA105 EHA105	TET-ORI	precise		0	
#011-36	LHAIUS	ILI-OKI	precise	12 ^b	U	precise
#050-1	EHA105	AMP-ORI	prooise	12	0	procisa
#050-1 #050-5	EHA105	AMP-ORI	precise precise	0	1 (A)	precise -61
#050-5 #050-6	EHA105	AMP-ORI	-1	1 (G)	0	-632
#050-9	EHA105	AMP-ORI	precise	12 ^b	0	precise
#050-10	EHA105	AMP-ORI	-		0	_
			precise	12 ^b		precise
#050-11	EHA105	AMP-ORI	precise	0	0	-629
#050-18	EHA105	AMP-ORI	-291	0	2 (GT)	-264
#050-24	EHA105	AMP-ORI	-10	0	0	-229
#050-27	EHA105	AMP-ORI	precise	12 ^b	0	precise
#050-30	EHA105	AMP-ORI	precise + ^d	1 (C)	0	-311
#050-35	EHA105	AMP-ORI	precise	12 ^b	0	precise
#050-37	EHA105	AMP-ORI	-75	0	4 (AGCT)	-464
#050-40	EHA105	AMP-ORI	precise	0	0	-130
#052-4	EHA105	AMP-ORI	-39	0	0	-644
#052-5	EHA105	AMP-ORI	precise	0	1 (T)	-92
#052-13	EHA105	AMP-ORI	precise	12 ^b	0	precise
#052-14	EHA105	AMP-ORI	precsie	12 ^b	0	precise
#052-16	EHA105	AMP-ORI	precise	0	1 (A)	-761
#052-19	EHA105	AMP-ORI	-1	0	0	-408
#052-24	EHA105	AMP-ORI	precise +d	1 (C)	13 bp of T-	-560
			Process		DNA or	
					binary	
					vector	
#052-26	EHA105	AMP-ORI	-2	0	sequence 0	-75
#052-29	EHA105	AMP-ORI	-24	0	0	-410
#052-30	EHA105	AMP-ORI	precise	0	0	-579
#052-38	EHA105	AMP-ORI	precise	12 ^b	0	precise
#052-43	EHA105	AMP-ORI	precise	12 ^b	0	precise
			•			-
#052-46 #052-47	EHA105	AMP-ORI AMP-ORI	precise	1 (A)	0 1 (A)	-43 743
#052-47 #052-48	EHA105 EHA105	AMP-ORI	precise	0	1 (A) 0	-743
			precise	12 ^b		precise
#052-49	EHA105	AMP-ORI	precise	0	0	-758
#052-50	EHA105	AMP-ORI	precise	12 ^b	0	precise
#052-51	EHA105	AMP-ORI	precise	12 ^b	0	precise
#052-54	EHA105	AMP-ORI	-342	0	1 (G)	-536

#052-58	EHA105	AMP-ORI	precise	2 (GA)	0	-234
#052-62	EHA105	AMP-ORI	precise	12 ^b	0	precise
#052-65	EHA105	AMP-ORI	-2	0	1 (A)	-25

^aRight border (RB) and left border (LB) numerical values represent the position in DNA relative to precise end; ^b12 bp can be a readthrough sequence of RB involved in microhomology with LB, or a precise RB joined to a precise LB end (i.e., no readthrough and microhomology); ^cThe two nucleotides after the precise RB (CA) can be a readthrough of a RB sequence involved in microhomology with a LB side, or precise RB without readthrough (CA comes from LB); ^dOne nucleotide after precise RB (C) can be a readthrough of RB sequence involved in microhomology with LB side, or precise RB without readthrough (C comes from LB sequence).

Supplemental Table 3. Sequenced T-DNA junctions of monomeric T-circles from *Arabidopsis efr-1* and Col-0 plants

Background	Sample No.	Strain	Construct	RB ^a	Microhomology	Filler DNA	LB ^a
efr-1							
	#022-2	EHA105	AMP-ORI	precise	12 ^b	0	precise
	#022-3	EHA105	AMP-ORI	precise	1 (A)	0	-22
	#022-4	EHA105	AMP-ORI	precise	12 ^b	0	precis
	#022-5	EHA105	AMP-ORI	precise	12 ^b	0	precis
	#022-6	EHA105	AMP-ORI	precise	12 ^b	0	precis
	#022-7	EHA105	AMP-ORI	precise	0	5 (TAATA)	precis
	#022-8	EHA105	AMP-ORI	-8	0	26 (TTAAT AGTTTAA ACTGAAG CGCAGAT)	precis
	#022-9	EHA105	AMP-ORI	precise	12 ^b	0	precis
	#022-10	EHA105	AMP-ORI	precise	12 ^b	0	precis
	#022-11	EHA105	AMP-ORI	precise	12 ^b	0	precis
	#022-12	EHA105	AMP-ORI	precise	12 ^b	0	precis
	#022-13	EHA105	AMP-ORI	precise	12 ^b	0	precis
	#022-14	EHA105	AMP-ORI	precise	12 ^b	0	precis
	#022-15	EHA105	AMP-ORI	precise	12 ^b	0	precis
	#022-16	EHA105	AMP-ORI	precise	12 ^b	0	precis
	#022-17	EHA105	AMP-ORI	precise	12 ^b	0	precis
	#022-18	EHA105	AMP-ORI	precise	0	1 (T)	-9
	#022-19	EHA105	AMP-ORI	precise	12 ^b	0	precis
	#022-20	EHA105	AMP-ORI	precise	12 ^b	0	precis
	#022-22	EHA105	AMP-ORI	precise	12 ^b	0	precis
	#022-23	EHA105	AMP-ORI	precise	12 ^b	0	precis
	#022-24	EHA105	AMP-ORI	precise	12 ^b	0	precis
	#022-25	EHA105	AMP-ORI	precise	12 ^b	0	precis
	#022-26	EHA105	AMP-ORI	-1	1 (G)	0	-16
	#022-27	EHA105	AMP-ORI	precise	0	1 (A)	-15
	#022-28	EHA105	AMP-ORI	precise	12 ^b	0	precis
	#022-29	EHA105	AMP-ORI	precise	12 ^b	0	precis
	#022-30	EHA105	AMP-ORI	precise	12 ^b	0	precis
	#022-31	EHA105	AMP-ORI	precise	12 ^b	0	precis
	#022-32	EHA105	AMP-ORI	precise	12 ^b	0	precis
	#022-33	EHA105	AMP-ORI	precise	12 ^b	0	precis
	#022-34	EHA105	AMP-ORI	-1	3 (TTG)	0	-9
	#022-35	EHA105	AMP-ORI	precise	12 ^b	0	precis
	#022-36	EHA105	AMP-ORI	precise	12 ^b	0	precis
	#022-37	EHA105	AMP-ORI	-13	4 (AAAC)	0	-18

#022-38	EHA105	AMP-ORI	precise	12 ^b	0	precise
#022-39	EHA105	AMP-ORI	precise	12 ^b	0	precise
#022-40	EHA105	AMP-ORI	precise	12 ^b	0	precise
#022-41	EHA105	AMP-ORI	precise	1 (A)	0	-6
#022-42	EHA105	AMP-ORI	precise	12 ^b	0	precise
#022-43	EHA105	AMP-ORI	precise	12 ^b	0	precise
#022-44	EHA105	AMP-ORI	precise	12 ^b	0	precise
#022-45	EHA105	AMP-ORI	precise	12 ^b	0	precise
#022-46	EHA105	AMP-ORI	precise	12 ^b	0	precise
#022-47	EHA105	AMP-ORI	precise	12 ^b	0	precise
#022-48	EHA105	AMP-ORI	precise	12 ^b	0	precise
#025-49	EHA105	AMP-ORI	precise	12 ^b	0	precise
#046-1	EHA105	AMP-ORI	precise	12 ^b	0	precise
#046-3	EHA105	AMP-ORI	precise	12 ^b	0	precise
#046-4	EHA105	AMP-ORI	precise	12 ^b	0	precise
#046-5	EHA105	AMP-ORI	precise	12 ^b	0	precise
#046-6	EHA105	AMP-ORI	precise	12 ^b	0	precise
#046-7	EHA105	AMP-ORI	precise	12 ^b	0	precise
#046-10	EHA105	AMP-ORI	precise	12 ^b	0	precise
#046-11	EHA105	AMP-ORI	precise	12 ^b	0	precise
#046-12	EHA105	AMP-ORI	precise	12 ^b	0	precise
#046-13	EHA105	AMP-ORI	precise	12 ^b	0	precise
#046-14	EHA105	AMP-ORI	precise	12 ^b	0	precise
#046-15	EHA105	AMP-ORI	precise	12 ^b	0	precise
#046-16	EHA105	AMP-ORI	precise	12 ^b	0	precise
#046-17	EHA105	AMP-ORI	precise	12 ^b	0	precise
#046-18	EHA105	AMP-ORI	precise	12 ^b	0	precise
#046-19	EHA105	AMP-ORI	precise	12 ^b	0	precise
#046-20	EHA105	AMP-ORI	precise	12 ^b	0	precise
#046-22	EHA105	AMP-ORI	precise	12 ^b	0	precise
#046-23	EHA105	AMP-ORI	precise	12 ^b	0	precise
#046-24	EHA105	AMP-ORI	precise	12 ^b	0	precise
#046-26	EHA105	AMP-ORI	precise	12 ^b	0	precise
#046-27	EHA105	AMP-ORI	precise	12 ^b	0	precise
#046-28	EHA105	AMP-ORI	precise	12 ^b	0	precise
#046-29	EHA105	AMP-ORI	precise	12 ^b	0	precise
#046-30	EHA105	AMP-ORI	precise	12 ^b	0	precise
#046-31	EHA105	AMP-ORI	precise	12 ^b	0	precise
#046-32	EHA105	AMP-ORI	precise	12 ^b	0	precise
#046-35	EHA105	AMP-ORI	precise	12 ^b	0	precise

#046-36	EHA105	AMP-ORI	precise	12 ^b	0	precise
#046-37	EHA105	AMP-ORI	-291	0	3 (GTC)	-15
#046-42	EHA105	AMP-ORI	precise	12 ^b	0	precise
#046-43	EHA105	AMP-ORI	precise	12 ^b	0	precise
#046-44	EHA105	AMP-ORI	precise	12 ^b	0	precise
#046-45	EHA105	AMP-ORI	precise	12 ^b	0	precise
#046-46	EHA105	AMP-ORI	precise	12 ^b	0	precise
#046-47	EHA105	AMP-ORI	precise	12 ^b	0	precise
#046-48	EHA105	AMP-ORI	precise	12 ^b	0	precise
#046-49	EHA105	AMP-ORI	precise	12 ^b	0	precise
#047-1	EHA105	AMP-ORI	precise	12 ^b	0	precise
#047-2	EHA105	AMP-ORI	precise	12 ^b	0	precise
#047-4	EHA105	AMP-ORI	precise	12 ^b	0	precise
#047-5	EHA105	AMP-ORI	precise	12 ^b	0	precise
#047-6	EHA105	AMP-ORI	precise	12 ^b	0	precise
#047-7	EHA105	AMP-ORI	precise	12 ^b	0	precise
#047-8	EHA105	AMP-ORI	precise	0	0	-581
#047-11	EHA105	AMP-ORI	precise	12 ^b	0	precise
#047-13	EHA105	AMP-ORI	precise	12 ^b	0	precise
#047-14	EHA105	AMP-ORI	precise	12 ^b	0	precise
#047-15	EHA105	AMP-ORI	precise	12 ^b	0	precise
#047-16	EHA105	AMP-ORI	precise	12 ^b	0	precise
#047-17	EHA105	AMP-ORI	precise	12 ^b	0	precise
#047-18	EHA105	AMP-ORI	precise	12 ^b	0	precise
#047-19	EHA105	AMP-ORI	precise	12 ^b	0	precise
#047-20	EHA105	AMP-ORI	precise	12 ^b	0	precise
#047-21	EHA105	AMP-ORI	precise	12 ^b	0	precise
#047-22	EHA105	AMP-ORI	precise	12 ^b	0	precise
#047-23	EHA105	AMP-ORI	precise	12 ^b	0	precise
#041-1	EHA105	AMP-ORI	precise	12 ^b	0	precise
#041-2	EHA105	AMP-ORI	precise	12 ^b	0	precise
#041-3	EHA105	AMP-ORI	precise	12 ^b	0	precise
#041-5	EHA105	AMP-ORI	precise	12 ^b	0	precise
#041-8	EHA105	AMP-ORI	precise	12 ^b	0	precise
#041-9	EHA105	AMP-ORI	precise	12 ^b	0	precise
#041-10	EHA105	AMP-ORI	precise	12 ^b	0	precise

Col-0							
	#021-1	EHA105	AMP-ORI	precise	12 ^b	0	precise
	#021-2	EHA105	AMP-ORI	precise	12 ^b	0	precise
	#021-5	EHA105	AMP-ORI	precise	12 ^b	0	precise
	#021-7	EHA105	AMP-ORI	precise	12 ^b	0	precise
	#021-8	EHA105	AMP-ORI	precise	12 ^b	0	precise
	#021-9	EHA105	AMP-ORI	precise	12 ^b	0	precise
	#021-10	EHA105	AMP-ORI	precise	12 ^b	0	precise
	#021-11	EHA105	AMP-ORI	precise	12 ^b	0	precise
	#021-12	EHA105	AMP-ORI	precise	12 ^b	0	precise
	#021-13	EHA105	AMP-ORI	precise	12 ^b	0	precise

^aRight border (RB) and left border (LB) numerical values represent the position in DNA relative to precise end; ^bMicrohomology of 12 bp nucleotides is true only of there were a readthrough of a RB sequence. Alternately, a precise LB and precise LB were joined without microhomology.

Supplemental Table 4. Sequenced T-DNA junctions from heterodimeric KAN-ORI and TET-ORI T-circles

G 1		RB-RB junction			LB-LB junction				
Sample No.	Constructs	RB (TET-ORI)	Microhomology	Filler DNA	RB (KAN-ORI)	LB (TET-ORI)	Microhomology	Filler DNA	LB (KAN-ORI)
#3	KAN-ORI and TET-ORI	-1	2 (CA)	0	precise	-105	0	1 (A)	-86
#4	KAN-ORI and TET-ORI	-231	2 (GA)	0	precise	-82	6 (TTCGGC)	0	-212
#5	KAN-ORI and TET-ORI	precise	0	0	precise	-98	3 (CAT)	0	-117
#6	KAN-ORI and TET-ORI	precise	1 (T)	U	-2	-81	2 (CG)	0	-29
#9	KAN-ORI and TET-ORI	precise	0	0	precise	-77	4 (TTAA)	0	-77
#10	KAN-ORI and TET-ORI	precise +2	2 (CA)	0	-1	-47	4 (ACAC)	0	-14
#10	KAN-ORI and TET-ORI	precise +2	0 (CA)	3 (ATA)		-4 <i>7</i> -66	5 (AATGT)	0	-14 -49
#11	KAN-ORI and TET-ORI	•		0 (A1A)	precise	-00 -41	` ′	0	-49 -41
		precise	0		precise .		4 (TTAA)		
#16	KAN-ORI and TET-ORI	precise	0	0	precise	-83	1(T)	9 bp T-DNA sequence	-20
#18	KAN-ORI and TET-ORI	-12	1 (A)	0	precise	NA	NA	ΝA	NA
#22	KAN-ORI and TET-ORI	precise	0	0	precise	-100	4 (TGTT)	0	-46
#24	KAN-ORI and TET-ORI	precise +2	2 (CA)	0	-1	-100	4 (AACA)	0	-1018
#25	KAN-ORI and TET-ORI	precise +2	2 (CA)	0	-1	-25	1 (T)	0	-86
#30	KAN-ORI and TET-ORI	precise	0	0	precise	NA	NA	NA	NA
#32	KAN-ORI and TET-ORI	precise	0	0	precise	-26	2 (TG)	0	-264
#37	KAN-ORI and TET-ORI	precise	0	0	-2	-78	4 (GTTA)	0	-1061
			RB-LB jun	ction			LB-RB jun	ection	
		LB (TET-ORI)	Microhomology	Filler DNA	RB (KAN-ORI)	RB (TET-ORI)	Microhomology	Filler DNA	LB (KAN-ORI)
#17	KAN-ORI and TET-ORI	precise	12**	0	precise	precise	12**	0	precise
			LB-RB jun	ction		RB-RB junction			
		LB (TET-ORI)	Microhomology	Filler DNA	RB (KAN-ORI)	RB (TET-ORI)	Microhomology	Filler DNA	RB (KAN-ORI)
#12*	KAN-ORI and TET-ORI	precise	12**	0	precise	precise	0	1 (A)	precise

^{*}The third junction (between two T-DNA LB sides) in T-circle #12 was not sequenced; **12 bp can be a readthrough sequence of RB involved in microhomology with LB, or a precise RB joined to a precise LB end (i.e., no readthrough and microhomology)

Supplemental Table 5. Characterization of T-circles isolated from *Nicotiana benthamiana* using the T-DNA binary vector pE4636

T-circle ID	Sequencin g Method	RB status	LB status	Microhomology at RB	Microhomology at LB	Filler DNA	Major rearrangements	Size (bp) ^{a,b}
M-1	Sanger	Precise	23 bp deletion	3 bp, but not directly at the border (TTGx)	3 bp (AAT)	303 bp from N. benthamiana	None	7814
K-10	Wide-Seq	327 bp deletion	4943 bp deletion	5 bp (GCGCC)	None	None	None	2241
J-1	Wide-Seq	Precise	89 bp deletion	None	None	None	None	6364
J-5	Wide-Seq	1 bp deletion	2072 bp deletion	None	None	1506 from pAtC58	None	6606
JYWT6	Sanger	Precise	?	None	None	None	From 97 to 1052 matched with expected T- circle 3720-2764 in reverse complement orientation	~ 7000
JYWT7	Sanger	Precise	484 bp deletion	None	None	736 bp from pAtC58	None	7674
JYWT8	Sanger	1 bp deletion	4352 bp deletion	2 bp	None	None	None	~3000
JYWT9	Sanger	7 bp deletion	4554 bp deletion	None	None	None	None	~3000
JYWT1 1	Sanger	1 bp deletion	4981 bp deletion	None	None	None	None	~2500
JY4	Sanger	Precise	?	None	None	801 bp from pE4636	Sequence ends with 801 bp from pE4636; needs Wide-Seq analysis	~12,000
JY6	Sanger	Precise	5972 bp deletion	None	None	None	The <i>bla</i> gene promoter and much of the <i>bla</i> gene are deleted, but there must be another full copy	~4000
4	Sanger	22 bp deletion	None	None	None	None	Inverted fragment insertion	~7500
10	WideSeq	327 bp deletion	4944 bp deletion	None	None	None	None	2241
4-3	Sanger	Precise	74 bp deletion	None	None	None	None	7437
4-10	Sanger	Precise	361 bp deletion	None	None	1 bp (T)	None	7151
4-7	Sanger	4 bp deletion	4610 bp deletion	None	None	None	None	2897
4-8	Sanger	83 bp deletion	3831 bp deletion	None	None	None	None	3622
4-12	Wide-Seq	456 bp deletion	4790 bp deletion	None	None	2667 bp from N. benthamiana	None	4932
4-14	Wide-Seq	458 bp deletion	4495 bp deletion	1 bp (T)	4 bp (ATCT)	None	1548 bp region from <i>Venus-intron</i> gene in inverted orientation	4106
4-23	Wide-Seq	362 bp deletion	4959 bp deletion	None	1 (T)	None	1328 bp from the <i>hptII</i> gene in inverted orientation	3520

4-20	Sanger	Precise	4816 bp deletion	None	None	None	None	2695
5-1	Sanger	3 bp deletion	4852 bp deletion	None	None	None	None	2656
5-2	Sanger	Precise	4801 bp deletion	None	None	None	None	2710
5-5	Sanger	Precise	88 bp deletion	2 bp (GA)	None	None	None	7424
6-2	Wide-Seq	Precise	4521 bp deletion	None	2 bp (TC)	1287 bp from the <i>hptII</i> gene, with part of the teminator	Inverted fragment insertion	4271
6-5	Sanger	Precise	5203 bp deletion	None	None	None	None	2308
6-6	WideSeq	Precise	4753 bp deletion	2 bp (GA)	None	3698 bp fragment from Venus cassette	inverted fragment insertion	6457
6-7	Sanger	Precise	5162 bp deletion	None	None	None	None	2349
6-8	WideSeq	Precise	4553 bp deletion	None	5 bp (AATGA)	1177 bp insertion (35S terminator)	Inverted fragment insertion	4263
6-9	Sanger	2 bp deletion	4291 bp deletion	None	None	2 bp (TG)	None	3220
6-15	Sanger	Precise	4622 bp deletion	2 bp (GA)	None	1 bp (T)	None	2890
6-19	Sanger	12 bp deletion	512 bp deletion	TTC vs. TTT	None	None	None	6978
6-24	Sanger	8 bp deletion	5326 bp deletion	None	None	1 bp (A) at the RB junction and 2 bp (AA) at the LB junction	Inverted fragment insertion	2889
6-28	Sanger	Precise	4842 bp deletion	None	2 bp (AA)	None	Inverted fragment insertion	2879
6-36	Sanger	Precise	220 bp deletion	None	None	None	None	7291
6-38	Sanger	322 bp deletion	4948 bp deletion	5 bp (GCGCC)	None	None	None	2241
6-39	Wide-Seq	Precise	4698 bp deletion	None	None	554 bp from pAtC58	Inverted fragment insertion	3368
6-41-21	Wide-Seq	1 bp deletion	2183 bp deletion	1 bp (G)	None	None	Inverted fragment from the binary vector	5964
6-42	Sanger	Precise	4222 bp deletion	1 bp (A)	None	None	None	3291
6-43-27	Sanger	18 bp deletion	4979 bp deletion	None	None	None	Inverted fragment (44 bp) insertion	2559
6-44	Sanger	138 bp deletion	446 bp deletion	4 bp (ATAA)	None	None	None	6927
6-51	Sanger	Precise	4990 bp deletion	2 out of 3 (TGA vs. TGC)	2 bp (AC)	None	Inverted fragment (290 bp) insertion	2811

^aSanger sequencing sizes are estimates based on the deletion sizes at the RB and LB ^bApproximate sizes are based on restriction endonuclease fragment sizes

Supplemental Table 6. Sequenced T-DNA junctions of monomeric T-circles from Arabidopsis ku80/efr-1 mutants

Sample No.	Strain	Construct	RB ^a	Microhomology	Filler DNA	LB ^a
#043-1	EHA105	AMP-ORI	Precise+2	4 (GACA)	0	-35
#043-2	EHA105	AMP-ORI	precise	12 ^b	0	precise
#043-3	EHA105	AMP-ORI	precise	12 ^b	0	precise
#043-4	EHA105	AMP-ORI	precise	12 ^b	0	precise
#043-5	EHA105	AMP-ORI	precise	12 ^b	0	precise
#043-6	EHA105	AMP-ORI	precise	12 ^b	0	precise
#043-7	EHA105	AMP-ORI	precise	12 ^b	0	precise
#043-8	EHA105	AMP-ORI	precise	12 ^b	0	precise
#043-9	EHA105	AMP-ORI	precise	12 ^b	0	precise
#043-10	EHA105	AMP-ORI	precise	12 ^b	0	precise
#043-11	EHA105	AMP-ORI	precise	12 ^b	0	precise
#043-12	EHA105	AMP-ORI	precise	12 ^b	0	precise
#043-15	EHA105	AMP-ORI	precise	12 ^b	0	precise
#043-16	EHA105	AMP-ORI	precise	12 ^b	0	precise
#043-17	EHA105	AMP-ORI	precise	12 ^b	0	precise
#043-18	EHA105	AMP-ORI	precise	12 ^b	0	precise
#043-19	EHA105	AMP-ORI	precise	12 ^b	0	precise
#043-20	EHA105	AMP-ORI	-294	1 (C)	0	-59
#043-21	EHA105	AMP-ORI	precise	12 ^b	0	precise
#043-22	EHA105	AMP-ORI	precise	12 ^b	0	precise
#043-23	EHA105	AMP-ORI	precise	12 ^b	0	precise
#043-24	EHA105	AMP-ORI	precise	12 ^b	0	precise
#043-26	EHA105	AMP-ORI	precise	12 ^b	0	precise
#043-27	EHA105	AMP-ORI	precise	12 ^b	0	precise
#043-28	EHA105	AMP-ORI	precise	12 ^b	0	precise
#043-29	EHA105	AMP-ORI	precise	12 ^b	0	precise
#043-31	EHA105	AMP-ORI	precise	12 ^b	0	precise
#043-32	EHA105	AMP-ORI	precise	12 ^b	0	precise
#043-33	EHA105	AMP-ORI	precise	12 ^b	0	precise
#043-34	EHA105	AMP-ORI	precise	12 ^b	0	precise
#043-35	EHA105	AMP-ORI	precise	12 ^b	0	precise
#043-38	EHA105	AMP-ORI	precise	12 ^b	0	precise
#043-39	EHA105	AMP-ORI	precise	12 ^b	0	precise
#043-40	EHA105	AMP-ORI	precise	12 ^b	0	precise
#043-43	EHA105	AMP-ORI	precise	12 ^b	0	precise
#043-44	EHA105	AMP-ORI	precise	12 ^b	0	precise
#043-45	EHA105	AMP-ORI	precise	12 ^b	0	precise
#043-46	EHA105	AMP-ORI	precise	12 ^b	0	precise
#043-47	EHA105	AMP-ORI	precise	12 ^b	0	precise
#045-1	EHA105	AMP-ORI	precise	12 ^b	0	precise
#045-2	EHA105	AMP-ORI	precise	12 ^b	0	precise

#045-3	EHA105	AMP-ORI	precise	12 ^b	0	precise
#045-4	EHA105	AMP-ORI	precise	12 ^b	0	precise
#045-5	EHA105	AMP-ORI	precise	12 ^b	0	precise
#045-6	EHA105	AMP-ORI	precise	12 ^b	0	precise
#045-8	EHA105	AMP-ORI	precise	12 ^b	0	precise
#045-9	EHA105	AMP-ORI	precise	12 ^b	0	precise
#045-10	EHA105	AMP-ORI	precise	12 ^b	0	precise
#045-11	EHA105	AMP-ORI	precise	12 ^b	0	precise
#045-14	EHA105	AMP-ORI	precise	12 ^b	0	precise
#045-15	EHA105	AMP-ORI	precise	12 ^b	0	precise
#045-16	EHA105	AMP-ORI	precise	12 ^b	0	precise
#045-17	EHA105	AMP-ORI	precise	12 ^b	0	precise
#045-18	EHA105	AMP-ORI	precise	12 ^b	0	precise
#045-20	EHA105	AMP-ORI	precise	12 ^b	0	precise
#045-21	EHA105	AMP-ORI	precise	12 ^b	0	precise
#045-22	EHA105	AMP-ORI	precise	12 ^b	0	precise
#045-24	EHA105	AMP-ORI	precise	12 ^b	0	precise
#045-25	EHA105	AMP-ORI	precise	12 ^b	0	precise
#045-27	EHA105	AMP-ORI	precise	12 ^b	0	precise
#045-28	EHA105	AMP-ORI	precise	12 ^b	0	precise
#045-29	EHA105	AMP-ORI	precise	12 ^b	0	precise
4 045-30	EHA105	AMP-ORI	precise	12 ^b	0	precise

^aRight border (RB) and left border (LB) numerical values represent the position in DNA relative to a precise end.

^bMicrohomology of 12 bp nucleotides is true only of there were a readthrough of a RB sequence. Alternately, precise RBs and precise LBs were joined without microhomology.

Supplemental Table 7. Bacterial strains used in this study

Strains & plasmids	Description/Use	Antibiotic resistance ¹	Reference
E. coli:			
DH10B	F- $mcrA$ $\Delta(mrr-hsdRMS-mcrBC)$ $\phi 80lacZ\Delta M15$ $\Delta lacX74$ $recA1$ $endA1$ $araD139$ Δ $(ara-leu)7697$ $galU$ $galK$ $\lambda-$ $rpsL(Str^R)$ $nupG$	None	Grant et al., 1990
E4	E. coli 2104 containing pPH1JI	Gent	Hirsch and Beringer, 1984
E1500	pUC18 with P _{virD} -VirD1-VirD2 ω mutation	Amp	Gelvin lab stock
E1727	pLAFR1 containing an <i>Eco</i> RI fragment containing a modified <i>picA</i> locus	Tet	Gelvin lab stock
E1745	5.5 kbp blunted <i>Eco</i> RI fragment of pE1500 cloned to the blunted <i>Pst</i> I site of pE1727	Amp, Tet	Gelvin lab stock
E1961	2.6 kbp <i>PstI</i> fragment containing the <i>sacRB</i> genes cloned into the <i>PstI</i> site of pBluescript KS-	Amp	Gelvin lab stock
E3052	EcoRI-SacII fragment containing the VirD2 gene cloned into the corresponding sites of pSAT6-nEYFP-C1	Amp	Gelvin lab stock
E3332	7.2 kbp <i>Xho</i> I fragment containing the <i>VirD</i> operon cloned into the <i>Xho</i> I site of pBluescript KS+	Amp	Gelvin lab stock
E3351	Klenow filled-in <i>Asp</i> 718 site of pBluescript KS+	Amp	Gelvin lab stock
E3353	3.27 kbp blunted <i>Sph</i> I-XhoI fragment of pE3332 cloned into the <i>Sma</i> I-XhoI sites of pE3351	Amp	Gelvin lab stock
E3355	HindIII fragment from pE3052 cloned into the HindIII site of pE3353	Amp	Gelvin lab stock
E3356	<i>Kpn</i> I deletion of pE3355 to create a non-polar deletion of <i>VirD2</i>	Amp	Gelvin lab stock
E3358	XhoI-NotI fragment from pE3356 cloned into the corresponding sites of pJQ200sk	Gent	Gelvin lab stock
E4329	pPZP-hpt-Venus-intron binary vector	Spec	Gelvin lab stock
E4579	pE4330 ligated to pUC19 at the <i>Sal</i> I and <i>Sac</i> I sites	Amp, Spec	This study
E4636	T-circle binary vector	Spec	This study
E4252	pRCS11 (TET-ORI; KS101)	Tet, Spec	This study
E4253 E4254	pTET-ORI modified RB region; KS102 TT3369; pAMP-ORI T-circle binary	Tet, Spec Amp, Spec	This study Singer et al., 2012
E4255	vector TT4500; pKAN-ORI T-circle binary vector	Kan, Spec	Singer et al., 2012
pEHC13	Cosmid clone of pTiBo542 Vir region		Hood et al., 1984
pJQ200sk	sacRB plasmid	Gent	Quandt and Hines, 1993
A. tumefaciens:			,
A136	Strain C58 cured of the Ti-plasmid	Rif	Watson et al., 1975
EHA105	Disarmed super-virulent strain	Rif	Hood et al., 1993
At1132	pE1745 in A136	Carb, Rif, Tet	Gelvin lab stock
At1136	Transconjugant from At1132 x E4	Carb, Rif	Gelvin lab stock
At1697	EHA105 with a non-polar VirD2 deletion	Rif	This study
At1710	pTiBo542-ΔVirD2 from At1697 with the VirD2 ω substitution in At1136 + pPH1JI	Carb, Gent, Rif, Spec	Gelvin lab stock

At1959	pTiBo542-ΔVirD2 from At1697 with the VirD2 ω substitution lacking pPH1JI	Carb, Rif	This study
At2120	EHA105(pBISN1, pKS102)	Kan, Rif, Spec	This study
At2121	At1959(pBISN1, pKS102)	Kan, Rif, Spec	This study
At2162	At1959(pBISN1, pRCS11)	Carb, Kan, Rif, Spec	This study
At2168	pRCS11 in At1959	Carb, Spec	This study
At2273	pE4636 T-circle binary vector in EHA105	Carb, Rif, Spec	This study
At2332	pE4636 T-circle binary vector in A1959	Carb, Rif, Spec	This study

¹Amp, ampicillin; Carb, carbenicillin; Gent, gentamicin; Kan, kanamycin; Rif, rifampicin; Spec, spectinomycin; Tet, tetracycline